JOURNAL OF BACTERIOLOGY, Dec. 2004, p. 8385–8400 Vol. 186, No. 24
0021-9193/04/$08.00+0 DOI: 10.1128/JB.186.24.8385–8400.2004

Transcriptomic and Proteomic Characterization of the Fur Modulon in the Metal-Reducing Bacterium *Shewanella oneidensis*

Xiu-Feng Wan,[1]†‡ Nathan C. VerBerkmoes,[2,3]† Lee Ann McCue,[4] Dawn Stanek,[1] Heather Connelly,[2,3] Loren J. Hauser,[3,5] Liyou Wu,[1] Xueduan Liu,[1] Tingfen Yan,[1] Adam Leaphart,[1] Robert L. Hettich,[2] Jizhong Zhou,[1] and Dorothea K. Thompson[1]*

Environmental Sciences Division,[1] Chemical Sciences Division,[2] and Life Sciences Division,[5] Oak Ridge National Laboratory, and Graduate School of Genome Science and Technology, University of Tennessee-Oak Ridge National Laboratory,[3] Oak Ridge, Tennessee, and The Wadsworth Center, New York State Department of Health, Albany, New York[4]

Received 29 March 2004/Accepted 26 August 2004

The availability of the complete genome sequence for *Shewanella oneidensis* MR-1 has permitted a comprehensive characterization of the ferric uptake regulator (Fur) modulon in this dissimilatory metal-reducing bacterium. We have employed targeted gene mutagenesis, DNA microarrays, proteomic analysis using liquid chromatography-mass spectrometry, and computational motif discovery tools to define the *S. oneidensis* Fur regulon. Using this integrated approach, we identified nine probable operons (containing 24 genes) and 15 individual open reading frames (ORFs), either with unknown functions or encoding products annotated as transport or binding proteins, that are predicted to be direct targets of Fur-mediated repression. This study suggested, for the first time, possible roles for four operons and eight ORFs with unknown functions in iron metabolism or iron transport-related functions. Proteomic analysis clearly identified a number of transporters, binding proteins, and receptors related to iron uptake that were up-regulated in response to a *fur* deletion and verified the expression of nine genes originally annotated as pseudogenes. Comparison of the transcriptome and proteome data revealed strong correlation for genes shown to be undergoing large changes at the transcript level. A number of genes encoding components of the electron transport system were also differentially expressed in a *fur* deletion mutant. The gene *omcA* (SO1779), which encodes a decaheme cytochrome *c*, exhibited significant decreases in both mRNA and protein abundance in the *fur* mutant and possessed a strong candidate Fur-binding site in its upstream region, thus suggesting that *omcA* may be a direct target of Fur activation.

A diverse array of prokaryotic organisms utilize Fur (the ferric uptake regulator) to control iron homeostasis at the level of transcription (6, 7, 9, 22, 24, 26, 37, 51, 61–63, 65, 68, 70). Iron is an important micronutrient that participates in many major cellular processes (e.g., respiration, enzyme catalysis, and gene regulation) (1); however, free Fe(II) can be detrimental because of its ability to catalyze Fenton reactions and the formation of highly reactive hydroxyl radicals (66). Consequently, the dynamics of intracellular iron concentrations must be precisely controlled and managed to prevent iron-induced oxidative stress due to excessive levels of free Fe(II).

Fur is an iron-responsive, homodimeric metalloprotein that complexes with Fe(II) to repress the transcription of genes or operons determining siderophore biosynthesis and transport in response to high intracellular Fe(II) concentrations (1, 20, 27). Fur accomplishes this repression by binding to a specific sequence element, the "Fur box", in the target promoters of iron-regulated genes, thus effectively blocking transcription by the RNA polymerase holoenzyme (3, 14, 15). In response to iron limitation, Fur no longer binds to the operator site, and transcription from target promoters resumes. Although Fur was initially defined as an iron response regulator of Fe acquisition systems, it has recently been shown to function as a pleiotropic regulator, involved in the control of such diverse cellular processes as acid tolerance (8, 22) and oxidative stress responses (28–30, 46, 63), chemotaxis (34), metabolic pathways (26, 59, 63), and virulence factor production (for a review, see reference 52).

Previously, the partial transcriptome analysis of a *fur* insertion mutant of the dissimilatory metal ion-reducing bacterium *Shewanella oneidensis* MR-1 (63), which possesses remarkably diverse respiratory capacities that have important implications with regard to the potential for bioremediation of metal contaminants in the environment, was described. Since the publication of the earlier study, sequence determination and closure of the *S. oneidensis* 5-Mbp genome was completed by The Institute for Genomic Research (TIGR) (32), making it feasible to conduct a global analysis of the dynamics of the MR-1 transcriptome in response to physiological or genetic perturbations. In the study reported here, we provide a comprehensive characterization of the *S. oneidensis* Fur modulon from the perspectives of both the transcriptome and the proteome. Comparison of whole-transcriptome data from DNA microarrays and proteome data obtained from direct analysis of whole-cell lysates using liquid chromatography-tandem mass spectrometry (LC-MS/MS) generally indicated good correlation

* Corresponding author. Mailing address: Environmental Sciences Division, Oak Ridge National Laboratory, P.O. Box 2008, Oak Ridge, TN 37831-6038. Phone: (865) 574-4815. Fax: (865) 576-8646. E-mail: thompsondk@ornl.gov.

† Xiu-Feng Wan and Nathan C. VerBerkmoes contributed equally to this work.

‡ Present address: Department of Computer Science, University of Missouri, Columbia, MO 65211.

between mRNA abundance levels and protein expression, particularly in cases where the transcript levels were high. In addition, MS-based proteome analysis detected protein products for a number of open reading frames (ORFs) that were designated pseudogenes in the published TIGR annotation and clearly identified a number of transporters, binding proteins, and receptors related to iron uptake not identified in previous *S. oneidensis* proteome studies (5, 16, 25, 41, 63, 67, 69). Application of the motif discovery programs Gibbs Recursive Sampler (35, 64) and MOTIF REGRESSOR (11) to genes showing coexpression patterns in the *fur* mutant revealed a putative consensus sequence for Fur binding in *S. oneidensis* and implicated a number of genes encoding hypothetical proteins in iron metabolism or iron transport-related functions.

MATERIALS AND METHODS

Bacterial strains, plasmids, and culture conditions. *S. oneidensis* strain DSP10 (63), a spontaneous rifampin-resistant derivative of *S. oneidensis* MR-1, was used as the parental (wild-type [WT]) strain for mutant generation and as the reference strain for microarray analysis. *Escherichia coli* S17-1/λ_{pir} (33) cells were used in conjugal transfer of the suicide plasmid construct. *S. oneidensis* and *E. coli* strains were grown in Luria-Bertani (LB) medium at 30 and 37°C, respectively. When needed, the growth medium was supplemented with the following antibiotics: for *E. coli* and *S. oneidensis*, 15 μg of gentamicin (GEN) per ml; for *S. oneidensis*, 10 μg of rifampin per ml. The suicide vector pDS3.1 was constructed in two steps, using as a template plasmid pCVD442, which was constructed by cloning the *sacB* gene on a PstI fragment from plasmid pUM24 (53) into plasmid pGP704 (39): (i) pDS3.0 was constructed by cloning the GEN resistance gene from vector pBSL142 (American Type Culture Collection, Manassas, Va.) into the EcoRV site of pCVD442; (ii) pDS3.1 was constructed by cloning the TA site and the *lacZ* gene from pGEM5fZ (Promega Corp., Madison, Wis.) into the SmaI site of pDS3.0.

For microarray analyses, *S. oneidensis* parental and mutant strains were grown in LB medium in the presence of 20 mM lactate at 30°C under aerobic or anaerobic (with 20 mM fumurate as the electron acceptor) conditions. For the aerobic conditions, cells were grown (60 ml in a 250-ml flask) with agitation (200 rpm). For the anaerobic conditions, the medium (80 ml in a 100-ml bottle) was purged with nitrogen gas and boiling for at least 30 min.

Generation of a *fur* deletion mutant. An *S. oneidensis* strain defective in the Fur regulatory protein (gene SO1937) was created using a PCR-based in-frame deletion strategy initially described by Link et al. (36). Briefly, oligonucleotide primers with complementary 5′ regions were used to generate two DNA fragments with 3′ staggered ends by asymmetric PCR using the following inside (I) and outside (O) specific primers (noncomplementary tag sequences are underlined): 1937-5I (5′-TGTTTAAACTTAGTGGATGGGGACTGTTGCTAGACCAATTTCTTCACC-3′), 1937-3I (5′-CCCATCCACTAAGTTTAAACAATAACTGCGAGCACAACGACG-3′), 1937-5O (5′-GCAAGTACAGCCGTTATTCACTCC-3′), and 1937-3O (5′-GTATCCAAAGGATGCAACTGG-3′). The PCR primers were designed so that the deletion maintained the original translational reading frame of ORF SO1937 (36). The two PCR products were then combined in a fusion reaction so that the overlapping ends were allowed to anneal together and serve as primers in the 3′ extension reaction of the complementary strands. In the final stage, the fusion molecule was amplified by PCR using the outer primer pair (1937-5O and 1937-3O) to obtain a tagged DNA fragment with an in-frame internal deletion. The internal fragment deleted from the *fur* locus consisted of 241 bp, which included the predicted DNA-binding domain and both metal-binding sites (48).

The mutated copy of the *fur* gene was then cloned into the suicide vector pDS3.1 (D. Stanek, and J. Zhou, unpublished data), which carries the *sacB* cassette and possesses a lambda-*pir*-dependent (R6K) origin of replication. The recombinant plasmid was introduced into a rifampin-resistant strain of *S. oneidensis* MR-1 by conjugation as described previously (63). Integration of the suicide construct into the chromosome was selected by GEN-rifampin resistance and confirmed by PCR amplification and sequencing. After integration of the suicide plasmid was verified, one of the resulting mutants was grown in LB broth without GEN and plated onto medium containing 5% sucrose. A fraction of the resulting sucrose-resistant colonies were screened by using colony PCR (72). Deletion of the *fur* locus in the final mutant strain was confirmed by DNA sequencing.

Microarray construction. The *S. oneidensis* microarray contained a total of 4,761 distinct elements, representing ~99% of the total protein-coding capacity of the MR-1 genome. Of the array elements that were spotted, 4,310 constituted PCR-amplified DNA fragments corresponding to unique segments of individual MR-1 ORFs, whereas gene-specific oligonucleotide probes (50-mers) were designed and synthesized for 451 predicted genes (9% of the total DNA probes arrayed) that did not yield either single products or any products in PCR amplifications. PCR primers and oligonucleotide probes were designed using the program PRIMEGENS (71). PCR products and oligonucleotides were printed in duplicate onto SuperAmine glass slides (TeleChem International, Inc.) as described previously (63). The microarray also consisted of 32 elements corresponding to *S. oneidensis* genomic DNA (positive controls) and 42 spots representing nine genes (amplicons) from *Arabidopsis thaliana* (negative controls).

RNA isolation, cDNA labeling, microarray hybridization, and scanning. Cultures of *S. oneidensis* wild-type and *fur* mutant strains were harvested at the midexponential point (optical densities at 600 nm [OD_{600}] of 0.6 under aerobic conditions and 0.25 under anaerobic conditions), and total cellular RNA was isolated using the TRIzol reagent (Invitrogen, Carlsbad, Calif.) according to the manufacturer's instructions. RNA samples were treated with RNase-free DNase I (Ambion, Inc., Austin, Tex.) to digest residual chromosomal DNA and then purified with the QIAGEN RNeasy Mini kit prior to spectrophotometric quantitation at 260 and 280 nm.

Fluorescein-labeled cDNA copies of total cellular RNA extracted from wild-type and mutant cells were prepared essentially as described previously (63), with the exception that Cy3/Cy5-dUTP (Perkin-Elmer/NEN Life Science Products, Boston, Mass.) was used in the first-strand reverse transcription (RT) reaction. Two sets of duplicate reactions were carried out in which the fluorescent dyes were reversed during cDNA synthesis to minimize gene-specific dye effects. The labeled cDNA probe was purified and concentrated as described previously (63).

For each growth condition tested, gene expression analysis was performed using six independent microarray experiments, including dye swapping, which yielded a total of 12 expression measurements per gene (three biological replicates, with each different mRNA preparation having four technical replicates). The two labeled cDNA pools (wild type and mutant) to be compared were mixed and hybridized simultaneously to the array in a solution containing 3× SSC (1× SSC is 0.15 M NaCl plus 0.015 M sodium citrate), 0.3% sodium dodecyl sulfate, 1 μM dithiothreitol (DTT), 40% (vol/vol) formamide, 0.8 μg of unlabeled herring sperm DNA (Gibco BRL)/μl, and 8.6% distilled H_2O. Hybridization was carried out in a 50°C water bath for 12 to 15 h. Following hybridization, the slides were washed and scanned as described elsewhere (63).

Quantitation of hybridization intensities and analysis. To determine the fluorescence intensity (pixel density) and background intensity, 16-bit TIFF scanned images were analyzed using the software ImaGene version 5.5 (Biodiscovery, Inc., Los Angeles, Calif.). Microarray outputs were first filtered to remove spots with poor signal quality by excluding those data points with a mean intensity of <2 standard deviations above the overall background for both channels (31). Empty spots and spots flagged as poor were removed from subsequent analyses by using ImaGene. Data transformation and normalization was carried out using GeneSite Light (Biodiscovery, Inc.). Normalized expression ratios were imported into ArrayStat (Imaging Research, Inc., Ontario, Canada) to determine the common error and to remove outliers. Only those genes with an expression ratio of ≥2 were included in further analyses (56).

Real-time RT-PCR analysis. To further validate the microarray data, nine ORFs exhibiting a range in expression levels from low to high (as identified by microarray analysis) were analyzed using real-time quantitative RT-PCR. The following genes were selected for comparative real-time RT-PCR analysis, and primer pairs (in parentheses) were designed using the program Primer3 (http://www-genome.wi.mit.edu/cgi-bin/primer/primer3_www.cgi): *crp* (5′-TGGTAAGCCAAAACCAGACC, 3′-GTCTTCACCAGCATGGATCA), *etrA* (5′-ACGATTGCAGTATGGGAACC, 3′-GCCTTTTTGAATGGGCTTCT), a DNA-binding response regulator (5′-ATGAAGCGATTCTCGACTCC, 3′-AACGGACATTGGGCTAAAAA), *tonB1* (5′-CAGGGTGAATCACATCAACG, 3′-TAACAGCGTTACGAGCAGCA), *exbB1*(5′-CATTCCTCGCCTTGATGATT, 3′-GGCGTAGCTCTTTAACCCAAG), *exbD1* (5′-ATTGCACTCGAGCATAAGCA, 3′-TAAACGCGGTTAAATCAGCA), *tonB2* (5′-CAAAGGGTCGTACCTCAACC, 3′-GAACGACATTGCCGTATCAA), *exbB2* (5′-TGATGATCGAGCGTTATTGG, 3′-GTGCGTACCAAGAGGTGGTT), and *exbD2* (5′-ACAAGCGACTTCGAAACCAT, 3′-TAGCTGTGACGCGTTCGATA). The primer pairs were designed to yield a PCR product ~100 bp in length.

The cDNA template for real-time RT-PCR was synthesized in a 20-μl final reaction volume containing 5 μg of total RNA, 2.5 mM random hexamers, 0.5 mM deoxynucleoside triphosphates, 10 mM DTT, 40 U of RNase inhibitor (Invitrogen), 1× first-strand buffer, and 200 U of Superscript II reverse tran-

scriptase. The quantitative PCR was carried out in an iCycler thermal cycler (Bio-Rad, Hercules, Calif.) in 50-μl reaction mixtures containing 1× PCR buffer, 1.5 mM $MgSO_4$, 0.1 mM deoxynucleoside triphosphates, 600 nM forward and reverse primers, 1× SYBR green I (Molecular Probes, Eugene, Oreg.), and 2 U of *Taq* DNA polymerase. The amplification quantification was conducted during the elongation step, and data analysis was performed using the software iCycle 2.3 version B according to the manufacturer's instructions. Standards for each gene of interest were obtained by amplifying the selected gene from *S. oneidensis* genomic DNA using the procedure described above but without SYBR green I. The PCR products were purified using a QIAGEN agarose gel extraction kit and quantified using a spectrophotometer. Purity was examined by measuring the absorbance ratio of 260 nm/280 nm. Molarity was converted to copy number using Avogadro's number, and standards were used to establish a standard curve consisting of seven points (in triplicate) serially diluted from 10^7 to 10^1 copies.

Within the same plate, three technical replicates were included for each of the three biological replicates. The *fur*/WT ratio for each biological replicate was calculated based on the average of the three technical replicates. The final *fur*/WT ratio and standard error were calculated by the three *fur*/WT ratios from the biological triplicates. The linear correlation between the quantitative-PCR and microarray data was performed based on the log mean values using SigmaPlot version 8.0 (SPSS Inc., Chicago, Ill.).

LC-MS/MS and data analysis. For high-performance LC (HPLC) coupled with electrospray ionization-MS/MS (referred to as LC-MS/MS), *S. oneidensis* parental and FUR2 strains were grown in 1-liter cultures (a total of 2 liters/strain) under aerobic conditions as described above, pelleted by centrifugation, washed twice in ice-cold 50 mM Tris (pH 7.5), and stored at −80°C until they were ready for analysis. For protein extraction, cell pellets were resuspended in ice-cold 50 mM Tris (pH 7.5) and disrupted by sonication. Unbroken cells were pelleted by centrifugation (5,000 × *g*; 15 min), and the suspension of membrane and soluble proteins was aliquoted into 1-ml tubes and frozen at −80°C until it was analyzed. For all LC-MS/MS analyses, aliquots of wild-type and FUR2 samples were quantitated for the total protein amount using the bicinchoninic acid protein assay reagent (Pierce Biotechnology, Inc., Rockford, Ill.). Equal quantities of protein from all samples were denatured with 6 M guanidine and 5 mM DTT at 60°C for 1 h and then diluted in 50 mM Tris (pH 7.5)–5 mM $CaCl_2$ to obtain a final guanidine concentration of 1 M. Sequencing-grade trypsin (Promega) was added at 1:100, and digestion reactions were run for 16 h. Trypsin was added a second time at 1:100, and digestion was run for another 6 h, followed by a final reduction step with 10 mM DTT for 1 h. Samples were immediately desalted with a C_{18} Sep-Pak (Waters, Milford, Mass.), concentrated using a centrifugal evaporator (Savant Instruments, Holbrook, N.Y.) to ~10 μg/μl, and filtered to remove insoluble material. For equivalent LC-MS/MS analysis (see below), great care was taken to load equal quantities of wild-type and mutant samples onto the LC-MS/MS system.

Proteomes of WT and *fur* mutant strains were analyzed by three different shotgun LC-MS/MS techniques: one-dimensional (1D) LC-MS/MS with five injections and five *m*/*z* ranges scanned, 2D LC-MS/MS with one injection and one *m*/*z* range scanned, and 2D LC-MS/MS with two injections and two *m*/*z* ranges scanned. One-dimensional LC-MS/MS experiments were performed with an Ultimate HPLC (LC Packings, San Francisco, Calif.) coupled to an LCQ-DECA ion trap mass spectrometer (Thermo Finnigan, San Jose, Calif.) equipped with an electrospray source. Injections were made with a Famos (LC Packings) autosampler onto a 50-μl loop. Peptides were injected onto a VYDAC 218MS5.325 (Grace-Vydac, Hesperia, Calif.) C_{18} column (300-μm inside diameter [i.d.] by 25 cm; 300 Å with 5-μm-diameter particles) at a flow rate of 4 μl/min and separated over 240 min from 95% H_2O–5% acetonitrile (ACN)–0.5% formic acid to 30% H_2O–70% ACN–0.5% formic acid. The peptides were eluted directly into an electrospray source (Thermo Finnigan) with 100-μm-i.d. fused silica. For all 1D LC-MS/MS data acquisition, the LCQ was operated in the data-dependent mode, where the top four peaks in every full MS scan were subjected to MS/MS analysis. Dynamic exclusion was enabled with a repeat count of 1 and an exclusion duration of 1 min. Five separate 50-μl injections of each sample were made, and five segmented *m*/*z* ranges were scanned to increase the total proteome coverage.

Two-dimensional LC-MS/MS experiments were performed on a Famos/Switchos/Ultimate 2D HPLC system (LC Packings) coupled to an LCQ-DECA ion trap mass spectrometer equipped with a Finnigan nanospray source. Sample and salt (ammonium acetate) injections were made with the Famos autosampler onto an LC Packings SCX column (500-μm i.d. by 15 mm), which sits on valve A of the Switchos system. Peptides that eluted from the SCX column were captured on an LC Packings precolumn (300-μm i.d. by 5 mm; 300-Å PepMap) on valve B. After being desalted on the precolumn, the precolumn flow was switched in line with a nano-resolving column (VYDAC 218MS5.07515 C_{18}; 75-μm i.d. by 15 cm; 300 Å with 5-μm-diameter particles) connected directly to a nanospray source (Thermo Finnigan). After injection and each subsequent salt step, a reverse-phase gradient was run for 160 min to elute the peptides into the mass spectrometer (with the same solvent system described above). The mass spectrometer was operated as described above, except that a dynamic exclusion repeat count of 2 was employed. For the one-*m*/*z*-range experiment, one 50-μl injection of each sample was made with one *m*/*z* range scanned (400 to 2,000 *m*/*z*) and 11 salt steps ranging from 20 mM to 2 M ammonium acetate. For the two-*m*/*z*-range experiment, a 50-μl injection was made, followed by eight salt bumps with the mass spectrometer scanning from 400 to 1,000 *m*/*z*. A second 50-μl injection was then made, followed by eight salt bumps with the MS scanning from 990 to 2,000 *m*/*z*.

The resultant MS/MS spectra from each LC-MS/MS analysis were searched with SEQUEST (18) against all predicted proteins from the *S. oneidensis* TIGR annotation (32) plus predicted proteins from the genome annotation performed at the Oak Ridge National Laboratory (ORNL). ORNL annotation methods use three different genome-modeling programs: Glimmer (13, 55), Critica (2), and Generation (http://compbio.ornl.gov). The results from all three algorithms were combined, followed by an automated resolution of overlapping genes, creating a final gene list. The database for proteome analysis was prepared by selecting those protein sequences identified by the ORNL team that were not included in the published TIGR protein translation files and appending the proteins to the TIGR database (M. Land, L. Hauser, and F. W. Larimer, personal communication). The raw output files were filtered and sorted with DTASelect (60) with the following criteria: DelCN of at least 0.8 and fully tryptic ends with cross-correlation (Xcorr) values of 1.8 for singly charged ions (+1), 2.5 for doubly charged ions (+2), and 3.5 for triply charged ions (+3). SEQUEST (18) produces a number of different scores, which can be used in the filtering processes; the Xcorr, or cross-correlation, value is the most commonly used score for filtering purposes. The three WT and FUR2 analyses were compared with the Contrast software package (60). A list was made of all proteins showing a significant change of at least 30% sequence coverage and/or four or more unique peptides between the WT and *fur* samples in all three replicate analyses.

Computational identification of putative Fur-binding sites and analysis of hypothetical proteins. MOTIF REGRESSOR (11) and Gibbs Recursive Sampler (35, 64) were both used to predict transcription factor-binding motifs upstream of differentially expressed *S. oneidensis* genes in FUR2. To facilitate motif searching using MOTIF REGRESSOR, the two microarray-based expression profiles generated under aerobic and anaerobic conditions were analyzed separately, i.e., only expression values for the aerobic condition were used or only expression values for the anaerobic condition were used. We selected the first 100 genes (showing the greatest up-regulated or down-regulated expression ratios) as "top" genes and the top 250 genes to confirm the motif searching. The top 30 potential regulatory sites from each prediction were selected.

The Gibbs Recursive Sampler program was used with (i) 16- and 17-bp models allowed to fragment up to 24 bp; (ii) up to two sites per sequence, where P(0 sites) = 0.1, P(1 site) = 0.8, and P(2 sites) = 0.1; (iii) a position-specific background model to account for variation in local base composition; and (iv) the Wilcoxon signed-rank test (64; http://bayesweb.wadsworth.org/gibbs/gibbs.html). The sequences used for alignment were intergenic regions ≥50 bp upstream of putative translation start codons, as defined by the *S. oneidensis* genome annotation (NC_004347 and NC_004349). Negative controls for the Wilcoxon test were randomly chosen from the set of *S. oneidensis* intergenic regions, provided that the sequence lengths matched those of the test sequences and excluded any sequence region that included a promoter for a gene that showed at least a twofold change in expression during aerobic or anaerobic growth of *S. oneidensis* FUR2 versus that of the WT strain. The Wilcoxon test calculates a P value for the motif, given the null hypothesis that the sequences under study (the test sequences) are no more likely to contain sites than the negative control sequences and also considering the ranks of the scores of the predicted sites in the motif. The program SCAN was used to identify sites from a database that were described by the motif (45). SCAN calculates a P value for each of the identified sites that reflects the probability that a site with that score or better would occur in a random database of the same size.

The locations of hypothetical proteins were predicted by using the program SOSUI (40). Probable operons were provided courtesy of TIGR (19).

RESULTS

Transcriptome analysis. The generation of a *fur* mutant strain (FUR1) of *S. oneidensis* by suicide plasmid integration into the gene was described previously (63). To create a ge-

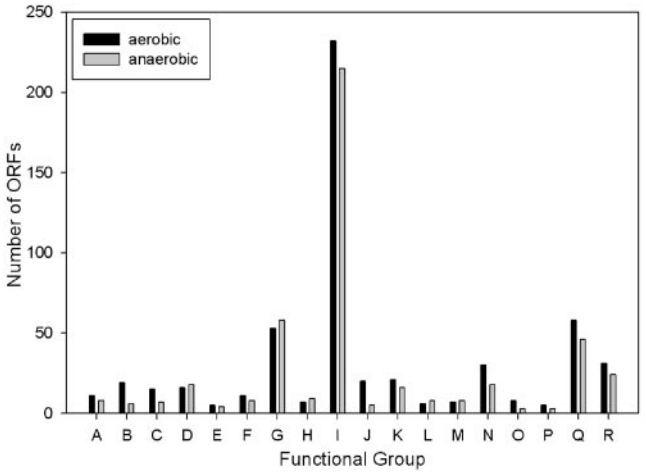

FIG. 1. Functional distribution of differentially expressed genes in the FUR2 strain. Each bar represents the number of ORFs showing significant changes in mRNA abundance in response to a *fur* deletion mutation under aerobic and anaerobic growth conditions. The ORFs are grouped in their corresponding functional and homology classes according to the TIGR annotation (http://www.tigr.org/tigr-scripts/CMR2/gene_attribute_results_org_or_role.dbi): (A) amino acid biosynthesis; (B) biosynthesis of cofactors, prosthetic groups, and carriers; (C) cell envelope; (D) cellular processes; (E) central intermediary metabolism; (F) DNA metabolism; (G) energy metabolism; (H) fatty acid and phospholipid metabolism; (I) hypothetical proteins; (J) other categories; (K) protein fate; (L) protein synthesis; (M) purines, pyrimidines, nucleosides, and nucleotides; (N) regulatory functions; (O) signal transduction; (P) transcription; (Q) transport and binding proteins; and (R) unknown function.

netically stable mutant defective in the Fur regulator, we employed a PCR-based in-frame deletion strategy to remove a 241-bp internal fragment in the *fur* locus containing the putative DNA-binding helix-turn-helix motif and both metal-binding domains (see Materials and Methods). The resulting deletion mutant, designated FUR2, exhibited a phenotype that was similar to the one previously reported for FUR1 (63). Global gene expression profiles of the FUR2 strain were compared to those of the DSP10 parental (wild-type) strain under both aerobic and anaerobic respiratory conditions (see Materials and Methods for details regarding replicates and data analysis).

In total, 567 and 479 genes were identified to be differentially regulated in response to a *fur* deletion under aerobic and anaerobic respiratory conditions, respectively (complete microarray datasets are available in Table S1 in the supplemental material [http://digbio.missouri.edu/~wanx/fur/fur.html]). Comparison of the two microarray datasets indicated that the expression levels for 334 genes were affected under both aerobic and anaerobic growth conditions. Responsive genes displayed a wide distribution among functional role categories, with 40 to 50% of these genes encoding hypothetical or conserved hypothetical proteins (Fig. 1). Other than genes with unknown functions, most of the ORFs showing significant differences in mRNA abundance levels in FUR2 relative to the wild-type strain are predicted to encode proteins involved in energy metabolism (53 [9.5%] and 58 [12.5%] under aerobic and anaerobic conditions, respectively) and transport and binding (58 [10.5%] and 46 [9.9%] under aerobic and anaerobic conditions, respectively). Another major category of affected *S. oneidensis* genes included those encoding regulatory functions (Fig. 1). There were 30 and 18 predicted regulatory genes that showed significant changes in expression in the FUR2 strain under aerobic and anaerobic conditions, respectively, and only 7 genes with annotated functions in regulation were differentially expressed under the two respiratory conditions.

Genes encoding transport and binding proteins. Selected genes showing at least a threefold difference in expression under one respiratory growth condition are listed in Table 1. Genes encoding transport and binding proteins with probable functions in iron acquisition and utilization were generally highly derepressed (≥10-fold increase in expression) in the FUR2 strain under both respiratory conditions. These genes coded for a bacterioferritin-associated ferredoxin (*bfd*; SO0583), TonB-dependent receptors (SO1482 and SO4743), a heme transport protein (*hugA*; SO3669), and a TonB1 transport system (*tonB1-exbB1-exbD1*; SO3670-SO3671-SO3672). Furthermore, expression of *ftn* (SO0139), which encodes the bacterial iron storage protein ferritin, was up-regulated ~6- and 9-fold under aerobic and anaerobic conditions, respectively (Table 1).

High-level constitutive expression of genes with putative functions in iron transport and assimilation agreed with results previously described for a *fur* insertion mutant of *S. oneidensis* (63), although transcriptome analysis with whole-genome arrays expanded the potential *S. oneidensis* Fur regulon to include previously unidentified members (e.g., *bfd*, *hugA*, *ftn*, and the *tonB1-exbB1-exbD1* operon). In addition, other iron transport and assimilation genes or operons exhibiting increases (2- to 44-fold) in transcript levels included *feoAB* (SO1783-SO1784), *hmuTUV* (SO3673 to -3675), *viuA* (SO4516), *irgA* (SO4523), and genes encoding a putative siderophore biosynthesis operon (SO3030 to -3032), a ferric alcaligin siderophore receptor (SO3033), and a TonB-dependent heme receptor (SO1580). Genes for a major facilitator family protein (SO0450), an ABC transporter with potential ATP-binding and permease activities (SO0821), and an outer membrane efflux family protein (SO0822) displayed moderate increases in transcription under both aerobic (three- to fivefold) and anaerobic (two- to threefold) growth conditions (Table 1). The substrate specificities of these putative transporters are unknown.

Interestingly, transcriptome analysis revealed that genes encoding a TonB2 transport system (the *exbB2-exbD2-tonB2* operon) showed only a 2.2-fold increase or no detectable change in mRNA levels in the FUR2 strain. This was in contrast to the substantial increases in expression (ranging from ~18- to 39-fold under aerobic respiration and from 30- to 35-fold under anaerobic respiration) observed for genes encoding the TonB1 Fe acquisition system (Table 1). Genes (*nosA*, SO0719, SO0737, SO0815, SO1102, SO1156, SO2427, SO2715, SO2907, and SO4077) coding for other putative TonB-dependent receptors showed no significant differences in mRNA expression levels in the *fur* deletion mutant under the growth conditions tested.

Genes with functions in energy metabolism. Genes with annotated functions in energy metabolism also showed altered expression profiles in the *fur* deletion mutant (Table 1). Generally, genes encoding components of electron transport systems in *S. oneidensis* were down-regulated in the FUR2 strain

TABLE 1. Subset of selected genes showing a ≥3-fold change in expression under at least one growth condition

Functional category	ORF	Gene product	Aerobic		Anaerobic	
			n^a	Mean[b] (*fur*/WT)	*n*	Mean (*fur*/WT)
Transport and binding proteins						
Cations	SO0139	Ferritin (*fin*)	8	6.41	10	9.2
	SO0583	Bacterioferritin-associated ferredoxin (*bfd*)	11	13.22	10	28.61
	SO0742	Iron(III) ABC transporter; ATP-binding protein	3	1.62	4	5.99
	SO0743	Iron(III) ABC transporter; permease protein	4	12.77	4	3.29
	SO0744	Iron(III) ABC transporter; periplasmic iron(III)-binding protein	9	0.96	5	4.13
	SO1111	Bacterioferritin subunit 2 (*bfr2*)	8	1.64	11	0.16
	SO1482	TonB-dependent receptor; putative	10	26.81	12	43.7
	SO1580	TonB-dependent heme receptor	4	2.48	6	6.36
	SO1783	Ferrous iron transport protein A (*feoA*)	4	11.19	7	5.04
	SO1784	Ferrous iron transport protein B (*feoB*)	8	3.54	12	7.49
	SO3030	Siderophore biosynthesis protein (*alcA*)	10	7.93	10	10.44
	SO3031	Siderophore biosynthesis protein; putative	10	3.41	8	3.46
	SO3032	Siderophore biosynthesis protein; putative	8	8.4	8	12.69
	SO3033	Ferric alcaligin siderophore receptor	8	6.41	10	13.49
	SO3669	heme transport protein (*hugA*)	6	26.45	10	74.96
	SO3670	TonB1 protein (*tonB1*)	10	19.02	11	33.16
	SO3671	TonB system transport protein ExbB1 (*exbB1*)	10	38.66	10	30.4
	SO3672	TonB system transport protein ExbD1 (*exbD1*)	6	17.65	7	34.82
	SO3673	Hemin ABC transporter; periplasmic hemin-binding protein (*hmuT*)	9	8.83	5	27.04
	SO3674	Hemin ABC transporter; permease protein (*hmuU*)	8	4.58	9	16.3
	SO3675	Hemin ABC transporter; ATP-binding protein (*hmuV*)	8	7.83	10	34.73
	SO4516	Ferric vibriobactin receptor (*viuA*)	8	8.21	6	8.77
	SO4523	Iron-regulated outer membrane virulence protein (*irgA*)	6	5.61	12	43.83
	SO4743	TonB-dependent receptor; putative	10	26.2	12	36.23
	SOA0153	Heavy-metal efflux pump; CzcA family	7	4.45	7	1.3
Porins	SOA0114	Outer membrane protein A (*ompA*)	6	4.29	7	1.07
Unknown substrate	SO0450	Major facilitator family protein	12	5.19	12	3.01
	SO0821	ABC transporter; ATP-binding/permease protein	11	5.03	12	2.14
	SO0822	Outer membrane efflux family protein	8	3.11	11	2.76
	SO1865	ABC transporter, ATP-binding protein	11	0.31	4	1.1
Energy metabolism						
Electron transport	SO0264	Cytochrome *c* (*scyA*)	7	2.29	4	0.19
	SO2916	Phosphate acetyltransferase (*pta*)	8	0.36	8	3.43
	SO4062	Polysulfide reductase; subunit A (*psrA*)	8	0.03	12	1.08
	SO1778	Decaheme cytochrome *c* (*omcB*)	11	0.19	12	0.25
	SO1779	Decaheme cytochrome *c* (*omcA*)	11	0.17	12	0.21
	SO1019	NADH dehydrogenase 1; C/D subunits (*nuoCD*)	11	0.92	8	0.22
	SO1020	NADH dehydrogenase 1; B subunit (*nuoB*)	8	1.33	5	0.18
	SO0846	Iron-sulfur cluster-binding protein NapH (*napH*)	4	17.93	10	1.41
	SO0847	Iron-sulfur cluster-binding protein NapG (*napG*)	4	9.46	9	1.05
	SO0849	NapD protein (*napD*)	2	38.69	8	0.82
	SO0845	Cytochrome *c*-type protein NapB (*napB*)	6	0.07	10	2.08
	SO0848	Periplasmic nitrate reductase (*napA*)	3	12.55	7	1.12
	SO1782	Decaheme cytochrome *c* MtrD (*mtrD*)	4	3.9	4	1.51
	SO1777	Decaheme cytochrome *c* MtrA (*mtrA*)	12	0.22	12	0.37
	SO3921	Periplasmic Fe hydrogenase; small subunit (*hydB*)	12	2.63	5	0.09
	SO3920	Periplasmic Fe hydrogenase; large subunit (*hydA*)	8	1.84	7	0.15
	SO2098	Quinone-reactive Ni/Fe hydrogenase; large subunit (*hyaB*)	2	0.22	6	0.16
	SO2099	Quinone-reactive Ni/Fe hydrogenase; small subunit precursor (*hoxK*)	12	0.27	4	1.51
	SO4591	Tetraheme cytochrome *c* (*cymA*)	12	0.73	7	0.29
	SO0809	Azurin precursor (*azu*)	4	10.26	3	2.15
	SO1364	Iron-sulfur cluster-binding protein	12	0.32	12	0.58
	SO1427	Decaheme cytochrome *c*	11	0.3	10	0.47
	SO2727	Cytochrome *c*3	8	1.51	5	0.12
	SO3420	Cytochrome *c′*	8	3.65	7	0.42

[a] Number of replicate data points (out of a total of 12) included in the analysis.
[b] Relative gene expression is presented as the mean ratio of the fluorescence intensity of the *fur* deletion mutant (FUR2 strain) to that of the parental strain (WT).

during growth under aerobic and/or anaerobic conditions. This was consistent with previous findings (63) and included a number of newly identified members of the Fur modulon. For example, members of two paralogous families of genes encoding decaheme cytochrome *c* proteins (32) consistently exhibited decreases in expression under both aerobic and anaerobic respiratory conditions (the respective decreases are given in parentheses): *omcA* (SO1779; 5.9- and 4.8-fold), *omcB* (SO1778; 5.3- and 4-fold), *mtrA* (SO1777; 4.5- and 2.7-fold), and a gene for an undefined decaheme cytochrome *c* (SO1427; 3.3- and 2.1-fold). MtrA is a member of the first group, including periplasmic proteins, and has been shown to be essential for Fe citrate and MnO_2 reduction by *S. oneidensis* (4), whereas OmcA and OmcB belong to the second family, which comprises likely outer membrane lipoproteins, and are known to be involved in the reduction of extracellular MnO_2 (44). Other genes encoding proteins of the electron transport system displayed down-regulated expression patterns in the FUR2 strain under both growth conditions and included *hyaB* (quinone-reactive Ni-Fe hydrogenase, large subunit), *hcp* (prismane protein), *cymA* (tetraheme cytochrome *c*), *ccmH* (cytochrome *c*-type biogenesis protein), *ccmE* (cytochrome *c* biogenesis protein), and gene SO1364, encoding an iron-sulfur cluster-binding protein. Genes *hydA* and *hydB* (which encode the large and small subunits, respectively, of periplasmic Fe hydrogenase), SO2727 (cytochrome c_3), and SO3420 (cytochrome *c*) showed decreased mRNA abundance levels only under anaerobic conditions.

Genes encoding regulatory or signal transduction functions. Genomic expression profiling indicated that 41 predicted regulatory genes (20.6% of the total genes assigned to this functional category) and nine members of two-component signal transduction systems were differentially expressed in the FUR2 strain compared to the parental strain (see Table S2 in the supplemental material [http://digbio.missouri.edu/~wanx/fur/fur.html]), thus suggesting that changes in the expression of other regulators likely contribute to the observed global transcriptional response. A number of *S. oneidensis* homologs for characterized transcriptional regulators exhibited differential expression in the FUR2 strain, including *crp* (SO0624), *irp* (SO2305), *cpxR* (SO4477), and *metJ* (SO4057). The response regulator CpxR, in combination with its cognate sensor kinase, CpxA, forms a two-component signal transduction system that senses a variety of envelope stresses and responds by activating the transcription of stress-combative genes (17). Our microarray results indicated that *cpxA* is up-regulated ~3-fold in the FUR2 strain under both aerobic and anaerobic growth. A concomitant increase (twofold) in the transcription of *cpxR* was observed under anaerobic conditions only, while mRNA abundance levels for *cpxR* remained essentially unchanged during aerobic growth (data not shown). In addition, a significant fourfold reduction in mRNA expression under aerobic respiration was observed for *etrA*, which encodes a putative electron transport regulator that shows ~74% primary sequence identity to *E. coli* Fnr (54). This expression pattern for *etrA* in a *fur* mutant agreed with our previous studies based on a partial genome array (63).

In addition to known transcriptional regulators, a number of differentially expressed genes encoded proteins showing homology to different families of transcriptional regulators (e.g., LysR and TetR protein families in particular), as well as sensory box proteins, response regulators, and sensor histidine kinases. One DNA-binding response regulator (SO2426) with an undefined function showed the most dramatic change in expression, with 30- and 26-fold increases in transcript levels under aerobic and anaerobic respiration, respectively.

Genes with unknown functions. The majority of differentially expressed genes in the *fur* mutant showed no similarity to sequences with known functions (Fig. 1). Table 2 lists only those genes with unknown functions exhibiting a ≥5-fold change in expression ratio under one or both growth conditions. The following ORFs were predicted to be organized in operons based on intergenic distances and coregulated expression patterns: (i) SO0447-SO0448-SO0449, (ii) SO0797-SO0798, (iii) SO1188-SO1189-SO1190, (iv) SO2684 to -2704, (v) SO3406-SO3407-SO3408, and (vi) SO3667-SO3668. Genes within the different predicted operons showed high-level induction in the *fur* mutant under both respiratory conditions, with the exception of genes in the probable SO2684-to-SO2704 operon, which showed increased transcription under aerobic conditions only (Table 2). In addition, the site locations of the proteins encoded by these functionally undefined genes were predicted using the computer program SOSUI (40), which discriminates transmembrane helical regions and thus indicates whether a protein is likely to be membrane associated rather than soluble (Table 2). Site location analysis indicated that 38% of the differentially expressed genes with unknown functions encoded membrane-associated proteins, with three of these proteins (SO0449, SO0975, and SO3407) predicted to contain eight transmembrane domains. For these genes and operons with unknown functions, this study provides the first evidence of their actual expression and suggests clues to their biological role in *S. oneidensis*.

Validation of transcriptome data by real-time RT-PCR. To independently validate the data generated by microarray hybridization, the expression levels of nine genes (*crp*, *etrA*, SO4157, *exbB2*, *exbD2*, *tonB2*, *tonB1*, *exbB1*, and *exbD1*) were also quantitated using real-time quantitative RT-PCR. The genes selected for comparative real-time RT-PCR analysis displayed a range of expression patterns (down-regulated, up-regulated, and no measurable change, as identified by microarray analysis) and included genes predicted to be organized within operons. Comparison of gene expression measurements by microarray hybridization and real-time RT-PCR indicated a high level of concordance ($r^2 = 0.86$; $n = 18$), despite quantitative differences in the levels of change (Fig. 2). For all nine genes tested, the general patterns of differential expression obtained from microarray analysis and RT-PCR were similar. However, RT-PCR showed 1,600 (±183)- and 372 (±19.3)-fold induction for *tonB1* and *exbB1*, respectively, under anaerobic respiration in contrast to the 33- and 30-fold induction observed in the microarray experiment, thus suggesting that DNA microarray analysis may underestimate changes in gene expression.

Proteome analysis. Whole-cell lysates of the *S. oneidensis* wild-type and FUR2 strains were digested with trypsin and analyzed by three similar shotgun LC-MS/MS methodologies (see Materials and Methods for details). The proteomes of the wild-type and FUR2 strains were compared by using qualitative analysis of the percent sequence coverage and the number

TABLE 2. Genes encoding hypothetical proteins that displayed a ≥5-fold change in expression in the FUR2 strain under at least one growth condition and identification of probable operons

ORF	Location[a]	Aerobic		Anaerobic	
		n[b]	Mean[c] (FUR2/WT)	*n*	Mean (FUR2/WT)
SOA0051	S		0.43	5	0.06
SOA0070	S	12	0.14	7	0.52
SO0324	S	8	0.07	12	0.92
SO0447[d]	M (3)	8	4.81	8	10.41
SO0448[d]	M (3)	5	4.45	7	6.37
SO0449[d]	M (8)	12	10.37	12	16.71
SO0786	S	2	5.77	4	2.33
SO0792	S	3	36.22	NA[e]	N/A
SO0797[f]	M (1)	9	3.97	9	3.77
SO0798[f]	S	10	26.73	6	103.09
SO0844	S	2	12.92	4	0.85
SO0908	S	7	5.34	5	2.82
SO0975	M (8)	8	0.2	10	0.32
SO1450	S	4	134.37	3	13.51
SO1454	S	3	0.17	4	0.56
SO1188[g]	M (3)	10	165.7	10	36.96
SO1189[g]	M (1)	12	18.98	11	29.51
SO1190[g]	M (1)	12	15.47	10	57.36
SO1572	S	3	6.26	4	11.43
SO1658	M (2)	3	64.91	4	2.57
SO1947	M (3)	8	0.18	6	0.63
SO2039	S	8	2.87	8	12.78
SO2425[h]	S	3	16.86	4	3.64
SO2671	S	6	5.17	3	0.58
SO2686[i]	S	12	10.37	12	16.71
SO2687[i]	S	10	12.15	4	1.21
SO2688[i]	S	10	6.39	5	1.26
SO2689[i]	M (1)	6	8.97	NA	N/A
SO2691[i]	S	6	5.38	4	0.792
SO2697[i]	S	12	7.52	5	0.99
SO2699[i]	S	6	5.09	3	1.022
SO2702[i]	S	10	25.22	6	0.04
SO2703[i]	S	2	8.35	NA	N/A
SO2735	M (1)	8	5.62	10	1.74
SO2929	S	8	0.17	11	0.83
SO2998	S	3	11.81	4	9.64
SO3003	S	2	9.93	4	3.17
SO3004	S	2	38.75	5	1.16
SO3011	S	3	19.98	2	1.07
SO3025	S	11	18.88	8	8.3
SO3062	M (3)	10	55.82	9	67.72
SO3344	M (4)	7	28.9	7	26.15
SO3369	S	2	176.27	4	5.99
SO3406[j]	M (3)	7	2.45	7	10.82
SO3407[j]	M (8)	11	24.48	11	27.73
SO3408[j]	M (4)	11	21.19	8	45.67
SO3587	M (1)	6	2.10	8	11.16
SO3667[k]	S	8	59.66	10	56.73
SO3668[k]	S	10	37.5	10	51.41
SO3676	M (1)	3	53.56	6	3.83
SO3891	M (1)	2	0.06	6	0.42
SO3913	S	6	2.28	4	6.45
SO4185	S	3	9.01	3	0.76
SO4700	S	11	8.67	1	9.33
SO4740	M (2)	3	77.83	9	13.15

[a] Predicted cellular location of the gene product, i.e., cytosol (soluble) (S) or membrane associated (M). The number given in parentheses next to the M designation refers to the number of transmembrane helices predicted using the computer program SOSUI (40).
[b] Number of replicate data points (out of a total of 12) included in the analysis.
[c] Relative gene expression is presented as the mean ratio of the fluorescence intensity of the FUR2 strain to that of the parental strain (WT).
[d] Probable operon SO0447-SO0448-SO0449.
[e] NA, not available.
[f] Probable operon SO0797-SO0798.
[g] Probable operon SO1188-SO1189-SO1190.
[h] Probable operon SO2426 (DNA-binding response regulator)-SO2425, SO2426 was up-regulated 30.2-fold and 25.9-fold under aerobic and anaerobic conditions, respectively.
[i] Probable operon SO2684 to SO2704.
[j] Probable operon SO3406-SO3407-SO3408.
[k] Probable operon SO3667-SO3668.

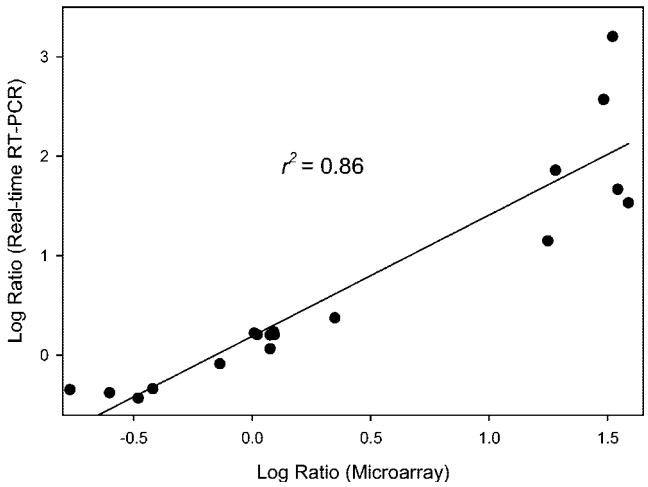

FIG. 2. Comparison of gene expression measurements by microarray hybridization and real-time quantitative RT-PCR. The changes in gene expression in a *fur* deletion mutant grown under both aerobic and anaerobic respiratory conditions were log transformed (in base 10). The real-time RT-PCR $\log_{10}$ ratio values were plotted against the microarray data $\log_{10}$ values. Comparison of the two methods indicated a high level of concordance (r^2 = 0.86).

of peptides identified in replicate shotgun LC-MS/MS analyses. Based on four replicate analyses of the same sample using 1D LC-MS/MS with multiple-mass range scanning, it was determined that a change of sequence coverage of 30% and/or ≥4 unique peptides was an appropriate cutoff to determine if a protein had a significant change in concentration between two samples above the general experimental variation (N. Ver-Berkmoes, unpublished data).

Table 3 presents the number of proteins identified from each experiment, the total amount of protein loaded onto the system, and the average percent sequence coverage per protein. While the total number of proteins identified per analysis

TABLE 3. Proteome analysis

Strain	Proteome method[a]	Total protein loaded (mg)	No. of proteins identified[b]	Avg sequence coverage (%)
FUR2	1D 5 *m/z*	5.0	490	19.78
	2D 1 *m/z*	0.5	765	17.95
	2D 2 *m/z*	1.0	807	18.39
WT	1D 5 *m/z*	5.0	555	21.90
	2D 1 *m/z*	0.5	611	18.13
	2D 2 *m/z*	1.0	673	18.20
Total		NA[e]	1,104[c]	19.06[d]

[a] Three different methods were used to analyze the proteomes of the *fur* deletion mutant (FUR2) and wild-type *S. oneidensis* strains: (i) 5 *m/z* refers to a five-part 1D-LC-MS/MS experiment, which involved five injections with four segmented *m/z* ranges and one full *m/z* range; (ii) 1 *m/z* refers to a single 2D-LC-MS/MS experiment that involved one injection and 11 subsequent salt steps analyzed by MS; (iii) 2 *m/z* refers to two 2D LC-MS/MS experiments, which included two injections each with 8 subsequent salt steps analyzed by MS over two *m/z* ranges.
[b] At least one peptide per protein was detected with Xcorrs of at least 1.8 (+1), 2.5 (+2), and 3.5 (+3).
[c] Sum of the numbers of nonredundant proteins identified for both WT and FUR2 samples.
[d] Average sequence coverage per protein detected.
[e] NA, not available.

changed dramatically, the average percent sequence coverage did not. We found that this variation was due mainly to a large number of proteins identified, with one or two peptides per protein; variations of this type were not considered in the final analysis. The three analyses for the wild type and mutant were compared with the Contrast (60) software, and the protein table was manually evaluated to determine proteins that showed reproducible changes above the stated cutoffs. The entire proteome data set is provided in Table S3 in the supplemental material (http://digbio.missouri.edu/~wanx/fur/fur.html). We then compiled the list of proteins and compared it with the transcriptome data (Table 4). In general, the results showed that the microarray expression data correlated well with the proteomics data for genes showing large-scale differences at the transcript level.

Correlation between transcriptome and proteome data. A total of 30 proteins from the 1,104 proteins comprising the proteome data set passed the base criteria of a reproducible change of at least 30% sequence coverage and/or four unique peptides. Of those 30 proteins, the expression patterns for 13 protein species correlated very well with the gene expression data, while 12 proteins determined to have large-scale changes in abundance by LC-MS/MS analysis did not show any significant change at the mRNA level, and 2 proteins showed an inverse correlation between microarray data and proteome data. Two ORFs (SO2304 and SO4422), whose encoded proteins were identified by proteomic analysis as showing significant changes in abundance, were originally annotated as pseudogenes and thus were not included on the microarray slides.

Genes showing strong correlation between microarray and LC-MS/MS analyses. Of the 13 proteins showing good correlation between the microarray and proteomics data, 11 were up-regulated and 2 were down-regulated in the *fur* deletion mutant relative to the parental strain. Of the 11 up-regulated proteins, 7 (SO1482, SO1580, SO3669, SO3914, SO4516, SO4523, and SO4743) were annotated as transporters or receptors involved in siderophore-mediated iron uptake. This is significant, because none of these proteins were identified in the previous study employing 2D polyacrylamide gel electrophoresis (PAGE) analysis (63), and it points to the advantage of LC-MS/MS techniques for detecting transport and binding proteins. Furthermore, this subset of proteins showed the largest changes in expression, with many being represented by $\geq$10 peptides in FUR2 and either 0 or 1 peptide in the wild type. The genes encoding these seven proteins also displayed large-scale differences (>5-fold induction) in expression, with the exception of two genes (SO1580 and SO3914) that exhibited only a 2- to 3-fold increase in mRNA abundance (Table 4).

Three conserved hypothetical proteins (SO1190, SO3667, and SO3668) were highly up-regulated in the *fur* deletion mutant and were found to have good correlation between the gene and protein expression data. SO3367 and SO3668 appear to be organized in an operon with SO3669 (a heme transport protein; *hugA*), which was also identified as being up-regulated in FUR2 by both microarray and LC-MS/MS analyses. It should be noted that the protein species encoded by gene SO3668 was detected with only three peptides in the FUR2 strain compared with zero in the wild type and thus did not meet our criteria for acceptance for the proteome data. However, the protein was included in Table 4 because of the location of its gene in a probable operon with SO3367 and SO3669 and its apparently coregulated expression (37.5-fold change), as identified by microarray analysis. Sequence analysis of the product of gene SO3668 revealed that the first half of the protein contains no trypsin cleavage sites, which possibly explains why <4 unique peptides were detected for this protein by the LC-MS/MS method.

Gene SO0798 was clearly identified as being up-regulated in the *fur* deletion mutant. A total of nine peptides were detected in FUR2 compared with no peptides identified in the WT sample. Microarray analysis indicated the same up-regulation, with a FUR2/WT expression ratio of 26.7. The public annotation (32) for this gene is a conserved hypothetical gene, but an alternative annotation performed at ORNL (see Discussion) identified this gene as having sequence similarity to a TonB-dependent receptor. The proteomic data provide preliminary evidence that this gene may indeed be a TonB-dependent receptor related to iron or other heavy-metal uptake. Two proteins, OmcA (SO1779) and OmcB (SO1778), showed down-regulated expression levels in the *fur* mutant, as identified by both DNA microarray and LC-MS/MS analyses (Table 4).

Genes showing significant expression changes by proteomic analysis but not by microarray analysis. Of the 30 proteins identified by proteomic analysis as changing in expression, 12 showed no substantial differences in mRNA levels by microarray hybridization. Six of these proteins were up-regulated in the FUR2 strain, and six were down-regulated, as determined by LC-MS/MS analysis. SO0520, annotated as a heavy-metal efflux pump protein, was identified with six peptides in the *fur* mutant sample and only one peptide in the wild-type sample, but the sequence coverage in both cases was very low due to the large size of the protein. Both SO2907 and SO4077 encode putative TonB-dependent receptors and showed a significant decrease in protein abundance in FUR2 compared with the wild type. For SO2907, 28 peptides were detected in the wild-type sample compared to only 4 in the *fur* mutant, whereas 8 peptides for SO4077 were detected in the wild type compared with 0 in FUR2. In both cases, the microarray data did not correspond to the proteomics data. The other eight proteins showed significant changes at the protein level and had unknown functions or had putative functions in energy metabolism, protein folding, and stabilization or in the biosynthesis of purines, pyrimidines, nucleosides, or nucleotides. For example, SO1377 (a conserved hypothetical protein) had 15 peptides detected in the wild-type sample, with none detected in the FUR2 analysis. Furthermore, this protein was repeatedly detected in the baseline proteome analysis of *S. oneidensis* in a previous study (69). Another hypothetical protein, SO3733, was detected repeatedly in the wild type, with a total of 12 unique peptides, but was never detected in the FUR2 strain. This protein was also repeatedly detected in a previous study of the wild-type strain (69). While the protein and mRNA levels do not seem to correlate for these two genes, their unknown functions and the fact that they are not expressed at a detectable level in the protein samples for the *fur* mutant make them interesting cases for further study.

Genes showing inverse correlation between proteome data and microarray analysis. Of the 30 genes identified by LC-MS/MS as showing significant changes in protein abundance,

TABLE 4. Comparison of transcriptome and proteome data

ORF[a]	Gene product	Proteomics								Microarray (mean[d] [FUR/WT])
		FUR2				WT				
		5 *m/z*[b]	1 *m/z*[b]	2 *m/z*[b]	Peptides[c]	5 *m/z*[b]	1 *m/z*[b]	2 *m/z*[b]	Peptides[c]	
Upregulated in FUR2										
SO0314	Ornithine decarboxylase; inducible (*speF*)	36.5	18.5	23.5	20	16.1	4.7	4.7	8	0.41[e]
SO0401	Alcohol dehydrogenase; zinc containing	69.4	63.5	54.3	14	0	3.6	0	1	NA[f]
SO0442	Phosphoribosylaminoimidazolecarboxamide formyltransferase/IMP cyclohydrolase (*purH*)	17.3	16.8	19.5	9	4.6	4.6	0	1	0.92[e]
SO0453	Peptidyl-prolyl *cis-trans* isomerase FkbP (*fkbP-1*)	0	11.7	42.3	4	0	0	0	0	1.17[e]
SO0520	Heavy-metal efflux pump; CzcA family	2.2	9.9	12.7	6	2.2	0	0	1	0.77[e]
SO0798	Conserved hypothetical protein	10.4	18.5	18.1	9	0	0	0	0	26.7
SO0958	Alkyl hydroperoxide reductase; C subunit (*ahpC*)	39.7	46.0	46.6	10	0	0	9.5	1	0.5[e]
SO1190	Conserved hypothetical protein	37.9	58.5	58.5	13	5.5	20	5.1	3	15.47
SO1482	TonB-dependent receptor; putative	37.9	34.8	26.5	22	0	0	0	0	26.81
SO1580	TonB-dependent heme receptor	14.7	12.9	24.8	12	0	3.1	0	1	2.48
SO2001	5′-nucleotidase (*ushA*)	13.2	16.0	14.1	8	6.7	4.2	4.2	2	1.11[e]
SO3667	Conserved hypothetical protein	37.3	42.7	31.4	10	7.0	0	0	1	59.66
SO3668	Conserved hypothetical protein	17.2	18.3	18.3	3	0	0	0	0	37.5
SO3669	Heme transport protein (*hugA*)	53.5	41.6	43.8	30	15.4	9.8	9.8	7	25.45
SO3914	TonB-dependent receptor; putative	19.5	11.0	24.1	16	10.4	0	0	4	2.83
SO4133	Uridine phosphorylase (*udp*)	42.1	43.3	43.3	6	6.7	9.5	21.4	3	0.75
SO4516	Ferric vibriobactin receptor (*viuA*)	10.8	10.8	25.3	8	0	0	0	0	8.21
SO4523	Iron-regulated outer membrane virulence protein (*irgA*)	69.0	56.7	54.4	34	17.8	4.2	6.8	4	5.61
SO4743	TonB-dependent receptor; putative	27.8	33.2	41.6	19	0	6.4	6.4	1	26.2
SO2304[g]	Alanine dehydrogenase	25.9	31.7	25.9	9	11.6	0	0	1	NA
SO4422[g]	TonB-dependent receptor; iron-siderophore receptor	44.6	42.5	35.5	11	0	13	13	2	NA
SO4422[g]	Similar to ferric aerobactin receptor	35	11.3	15.8	8	0	0	0	0	NA
Downregulated in FUR2										
SO1377	Conserved hypothetical protein	0	0	0	0	23.3	26.7	25.5	15	1.47[e]
SO1778	Decaheme cytochrome *c* (*omcB*)	0	0	0	0	9.8	15.5	17.7	11	0.19
SO1779	Decaheme cytochrome *c* (*omcA*)	0	0	0	0	4.2	12.5	13.6	6	0.17
SO2363	Cytochrome *c* oxidase; cbb3-type; subunit II (*ccoO*)	0	8.7	19.7	2	22.1	47.6	39.4	8	0.94[e]
SO2907	TonB-dependent receptor domain protein	4.5	10.5	4.3	4	29.6	37.1	40.2	28	1.32[e]
SO3733	Hypothetical protein	0	0	0	0	21.5	8.0	13.1	12	0.94[e]
SO4077	TonB-dependent receptor, putative	0	0	0	0	11.9	15.4	17.4	8	0.97[e]
SOA0048	Prolyloligopeptidase family protein	0	0	0	0	6.3	10.6	6.0	7	1.24[e]

[a] ORFs are presented that show a 30% change in sequence coverage or a difference of four or more unique peptides.

[b] 5 *m/z* refers to the percent sequence coverage from a five-part LC-MS/MS experiment covering the entire mass spectrum in five separate steps; 1 *m/z* refers to the percent sequence coverage from a single 2D LC-MS/MS experiment that involved one injection and 11 subsequent salt steps analyzed by MS; 2 *m/z* refers to the percent sequence coverage from two 2D LC-MS/MS experiments, which included two injections each with eight subsequent salt steps analyzed using MS over two *m/z* ranges.

[c] Total number of unique peptides detected per gene product by triplicate LC-MS/MS analysis.

[d] Relative gene expression is presented as the mean ratio of the fluorescence intensity of the FUR2 strain to that of the parental strain (WT).

[e] Change in expression was <2-fold.

[f] NA, not available.

[g] ORFs originally annotated by TIGR as pseudogenes whose expression was verified by proteomics.

two had inverse correlation with the microarray data. Proteins encoded by SO0314 (ornithine decarboxylase) and SO0958 (alkyl hydroperoxide reductase, C subunit) were both found to be significantly up-regulated in the FUR2 proteome. However, the corresponding genes were found to be down-regulated in the *fur* mutant sample by microarray analysis, with FUR2/WT ratios of 0.41 (SO0314) and 0.50 (SO0958).

Verified expression of proteins from pseudogenes. A protein sequence database based on the *S. oneidensis* MR-1 genome was constructed from two sources for our proteomic studies. This database included 4,778 protein sequences from the TIGR annotation (http://www.tigr.org/; 32), plus an additional 355 protein sequences provided by the Genome Analysis and System Modeling Group in the Life Sciences Division at ORNL. These 355 additional sequences consisted largely of the protein translations of ORFs annotated as pseudogenes by TIGR. Putative or partial translations of pseudogenes are not typically included in protein databases released by genome projects.

Proteome analysis of the *S. oneidensis* FUR2 and WT strains revealed that nine ORFs (see Table S4 in the supplemental material [http://digbio.missouri.edu/~wanx/fur/fur.html]) previously annotated as pseudogenes were expressed and detected with high confidence (i.e., at least two unique peptides identified per protein). However, many more proteins were detected with single-peptide identifications. Of particular interest were the following two genes that were found to be highly expressed in the *fur* deletion mutant but not in the wild-type strain: SO2304, annotated as an alanine dehydrogenase with an authentic point mutation, and SO4422, annotated as a siderophore receptor gene with one or more frameshifts (Table 4). Interestingly, the ORNL annotation predicted two ORFs in place of SO4422: a TonB-dependent receptor-iron siderophore receptor and a ferric aerobactin receptor. The protein products for these genes were easily identified in FUR2 ($\geq$8 peptides) but were either detected at very low levels or not at all in the wild-type strain ($\leq$2 peptides). Transcript expression data were not generated for these genes, because pseudogenes were not included in the fabrication of *S. oneidensis* whole-genome microarrays.

The remaining seven proteins identified showed no significant difference in sequence coverage or the number of peptides detected between the FUR2 and WT strains. These genes are still of interest due to the fact that the proteomics data verified their expression despite the apparent frameshifts and/or point mutations identified in the genome sequence that resulted in their annotation as pseudogenes. These seven proteins are encoded by SO0590, annotated as a phosphatidylserine decarboxylase (ORNL gene 700, identified with a total of 41.2% sequence coverage and 5 unique peptides); SO3130, a glutamate tRNA synthetase catalytic subunit (ORNL genes 1951 and 1952; 16.9% coverage with 2 peptides and 24% coverage with 2 peptides, respectively); SO2937, a putative ribosomal large-subunit pseudouridine synthase (ORNL gene 2085; 9.6% coverage and 2 peptides); SO2756, a probable peroxidase (ORNL gene 2202; 81.4% coverage and 12 peptides); SO3798, a hypothetical protein (ORNL gene 3461; 18.7% coverage and 2 peptides); SO1211, peptide chain release factor 3 (ORNL gene 4738; 12% coverage and 2 peptides); and SO1900, a putative acyl-coenzyme A synthetase (ORNL gene 5161; 11.8% coverage and 3 peptides). In light of these findings, we examined these genes in more detail. Of primary interest was SO4422, initially identified as a pseudogene by TIGR and as two proteins in the ORNL annotation due to a frameshift in the middle of the gene. Proteome analysis clearly revealed the expression of the intact gene product, since numerous peptides were detected from before and after the frameshift. The question this poses for SO4422, as well as others in this list, is how these genes are being expressed when sequence data indicate that they are likely pseudogenes with premature stops or frameshifts. SO1900 and SO3789 seem to be intact, despite their original annotation as pseudogenes, while for the remaining genes listed above, the most likely explanation may be sequencing errors in the final compiled genome DNA sequence or differences between the sequenced strain and individual laboratory strains. These new findings emphasize the value of using proteomic analyses to verify genome annotations and suggest that it may be useful to provide, in some form, potential protein translations of pseudogenes for proteome analyses.

Computational prediction of *S. oneidensis* Fur-binding consensus motif. To predict genes directly regulated by Fur, regions upstream of *S. oneidensis* ORFs showing differential expression in the *fur* deletion mutant, as identified by microarray analysis, were analyzed for transcription factor DNA-binding motifs using the Gibbs Recursive Sampler (35, 64) and MOTIF REGRESSOR (11) programs. The Gibbs Recursive Sampler (see Materials and Methods) was first applied to the intergenic regions upstream of *S. oneidensis* genes that displayed at least a fivefold change in mRNA abundance between the FUR2 and WT strains during aerobic or anaerobic growth. Several of these genes are arranged in likely operons; thus, this set included 94 unique intergenic regions of at least 50 bp, representing promoters for 150 *S. oneidensis* genes. Because the changes in gene expression observed in the microarray experiments may be attributable to more than one transcription regulatory factor, we initially searched for two motif types simultaneously. Multiple runs of Gibbs sampling analyses consistently identified a single significant 21-bp palindromic motif. Sites for this motif were observed in 71 of the 94 intergenic regions at least once in the Gibbs sampling frequency solutions. Because the initial Gibbs sampling runs identified at most a single significant motif, in the second round of Gibbs sampling, we searched for a single motif in the reduced data set of 71 intergenic sequences. We again performed multiple runs and, in addition, performed the Wilcoxon signed-rank test. A single statistically significant motif ($P < 0.000065$) was reproducibly identified, with sites in 30 of the sequences (Table 5). Considering the probable operon structure of these genes in the *S. oneidensis* genome, the predicted sites likely regulate the expression of at least 50 genes (Table 5).

By comparing the expression of a *fur* deletion mutant to that of the wild-type strain using microarray expression profiling, we expected to observe altered expression of Fur-dependent genes and thus to identify Fur-binding sites via the motif-finding methods described above. However, as a step toward confirming the identity of the cognate transcription factor for the predicted sites, we scanned a database of 654 experimentally verified *E. coli* binding sites for 79 known *E. coli* transcription factors with the palindromic-motif model found by

TABLE 5. Predicted motifs for individual genes[a]

Putative functional category	ORF	Gene product	Anaerobic		Aerobic		Pos[b]	Predicted binding site[c]	Prob[d]	Putative operon
			n	Mean (FUR2/WT)	*n*	Mean (FUR2/WT)				
Cellular processes										
Adaptations to atypical conditions	SO2355	Universal stress protein family	11	0.43	11	0.13	−65	atcggTTTTGAAAAGAGTTTTGATCTagaac	0.82	
Energy metabolism										
Electron transport	SO1779	Decaheme cytochrome *c* (*omcA*)	12	0.21	11	0.17	−43	acgacTAATGAGATTTGTTCTTATTTgatat	0.97	
	SO1782	Decaheme cytochrome *c* MtrD	4	1.51	4	3.90	−349	actggTAACGATAATAGTTTTCAATTgtgtt	0.99	SO1782-81-80
	SO4062	Polysulfide reductase; subunit A (*psrA*)	12	1.08	8	0.03	−234	acgatTTTTTAGAACAATTTTAACTTttagt	0.78	SO4062-61-60
Sugars	SO1755	Phosphoglucomutase/phosphomannomutase family protein	8	3.56	4	5.47	−9	aaggtAATTGAAAATGATTTTCACTGaggca	0.99	
Hypothetical proteins	SO0447	Hypothetical protein	8	10.41	8	14.81	−126	aatctTATTGCGAACTATTCTCATCAgtgct	0.99	SO0447-48-49
	SO0798	Conserved hypothetical protein	6	103.1	10	26.73	−41	aaatcAAATAATAACAATTCTCATTTacata	0.98	SO0798-97
	SO0799	Conserved hypothetical protein	5	3.05	5	2.19	−87	tatgtAAATGAGAATTGTTATTATTTgattt	0.98	
	SO1188	Conserved hypothetical protein	10	165.7	10	36.96	−164	atactTTTTGATAATAAATATCATTTactat	0.93	SO1188-89-90
	SO2039	Conserved domain protein	8	12.78	8	2.87	−23	ccattAAATGCGAATAATTAGCAATTaattc	0.99	
	SO3025	Conserved hypothetical protein	11	18.88	8	8.3	−199	ttggtAAATGACAATAGTTGTCATTTgagag	1.00	
	SO3027	Hypothetical protein	7	2.97	7	1.23	−316	ctctcAAATGACAACTATTGTCATTTaccaa	1.00	
	SO3406	Hypothetical protein	7	10.82	7	21.45	−252	aatgcAAATGATATTGTTTATCATTTaaatt	1.00	SO3406-07-08
	SO3062	Hypothetical protein	9	67.72	10	55.82	−46	aatttTGTTGAGAACAATTCTCATCTaaatt	1.00	
	SO3344	Hypothetical protein	7	26.15	7	28.9	−23	actttAAATGATAATGATTATCAGTTaaggc	1.00	
	SO4700	Hypothetical protein	11	8.67	11	9.33	−65	atcgcAAATCAAATCCATTCTCATTAatgat	0.98	
	SO4740	Conserved hypothetical protein	9	13.15	3	77.83	−39	aatttTAATGAGAATTGTTATCATCTaatta	1.00	
Protein fate										
Degradation of proteins, peptides, and glycopeptides	SO0445	HflC protein, putative	5	1.38	5	2.41	−186	agcacTGATGAGAATAGTTCGCAATAagatt	0.99	
Transport and binding proteins										
Cations	SO0139	Ferritin (*ftn*)	10	9.2	8	6.41	−112	tgaacAAATGAAAATCATTTTTATCAactaa	0.99	
	SO0583	Bacterioferritin-associated ferredoxin (*bfd*)	10	28.61	11	11.22	−34	attgcATTTGATAAGCGTTTTCATTTagaat	0.99	
	SO1111	Bacterioferritin subunit 2	8	1.64	8	0.16	−104	agcgaTAATGAGAATGCTTTTAATTAttaag	0.98	SO1111-12
	SO1482	TonB-dependent receptor; putative	12	43.7	10	25.81	−28	aaagaGGATGGAAATCATTATCATTCgcaac	0.93	
	SO1580	TonB-dependent heme receptor	6	6.36	4	2.48	−6	aaactATGTGAGAATTATTCTCATCTttggc	0.99	
	SO1783	Ferrous iron transport protein A (*feoA*)	7	5.04	4	11.19	−100	aacacAATTGAAAACTATTATCGTTAccagt	0.99	*feoAB*
	SO3030	Siderophore biosynthesis protein (*alcA*)	10	10.44	10	7.93	−187	cctgcAGATGAGAACGATTTGCATTTataat	1.00	*alcA*-SO3031-32
	SO3669	Heme transport protein (*hugA*)	10	74.96	6	25.45	−148	atcgcAAATGATAATGATTTCTATTTgatca	0.92	SO3669-68-67
	SO3670	TonB1 protein (*tonB1*)	11	33.16	10	19.02	−76	tgatcAAATAGAAATCATTATCATTTgcgat	0.92	*tonB1-exbB1-exbD1*
	SO4516	Ferric vibriobactin receptor (*viuA*)	6	8.77	8	8.21	−79	aatgtAAATGATATTGGTTATCAATTgcgat	0.99	
	SO4523	Iron-regulated outer membrane virulence protein (*irgA*)	12	43.83	6	5.61	−23	tccggTATTGAAAATTATTATCATTTagaaa	1.00	
	SO4743	TonB-dependent receptor; putative	12	36.23	10	26.20	−95	accttAAATAAAAACAATTCTTATTTatatt	0.98	
Additional genes with sites that match the motif										
	SO4196	Hypothetical protein	4	1.84	6	1.72	−236	accgtGATTGATAACACTTTTCTTTTcagga[e]	0.90	
	SO4197	*S*-adenosylmethionine 2-demethylmenaquinone methyltransferase (*menG-2*)	12	0.91	12	0.72	−69			
	SO3714	Putative sugar-binding protein	8	0.70	10	0.67	−318	tttgaAACTGATAACCGTTTTGATCAcattg[e]	0.88	
	SO3715	Oxygen-insensitive NAD(P)H nitroreductase	12	0.79	12	1.16	−73			
	SO0230	Ribosomal protein S10	9	1.34	12	0.86	−119	gaattAAATGATAAGTCTTTGAACTTatcat[e]	0.84	
	SO0744	Iron(III) ABC transporter; periplasmic iron(III)-binding protein	5	4.13	9	0.96	−55	ttcgaAACTGATAACTATTATCATTAatagt[f]		
	SO2841	Hypothetical protein	11	1.39	11	2.03	−39	tagttGACTGATAATAGTTTTCATTTagaat[f]		

[a] Upstream sequences of genes exhibiting ≥5-fold change in expression were analyzed for putative regulatory motifs using Gibbs Recursive Sampler.
[b] Position of the putative regulatory site relative to the translation start codon of the gene.
[c] Binding site is capitalized.
[d] Posterior probability that the site is described by the motif model.
[e] Additional sites predicted by Gibbs sampling in randomly chosen negative control sequences during the Wilcoxon test. Intergenic sequences upstream of SO4196-SO4197, SO3714-SO3715, and SO0230 were included during Gibbs sampling as negative controls for the Wilcoxon signed-rank test, because these genes did not exhibit ≥2-fold change in expression as determined by microarray analysis.
[f] Additional sites predicted ($P < 0.05$) by using the motif model in Fig. 3 to SCAN the set of intergenic sequences upstream of genes that exhibit an expression ratio of ≥2-fold.

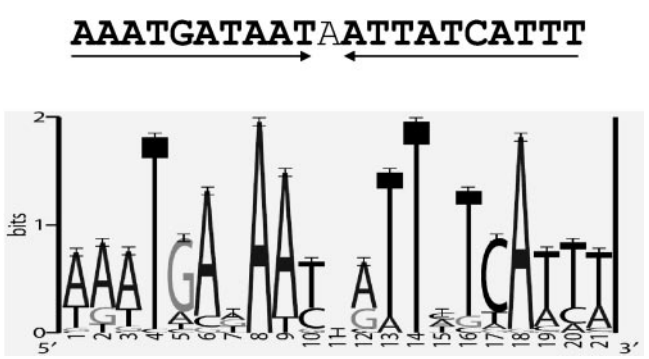

FIG. 3. Identification of a predicted consensus Fur-binding motif in *S. oneidensis* MR-1 using computational methods. A sequence logo representation (57) of a palindromic-motif model was derived based on only those sites listed in Table 5 that are directly upstream of genes exhibiting differential expression in response to a *fur* deletion mutation. The error bars indicate standard deviations of the sequence conservation.

Gibbs sampling (see Materials and Methods). At a *P* value of <0.1, SCAN identified seven *E. coli* Fur-binding sites and no binding sites for other known *E. coli* transcription factors.

To compare the results of Gibbs sampling with those generated by other motif-finding methods, MOTIF REGRESSOR was applied to two separate data sets: (i) sequences upstream of genes displaying differences in transcript levels under anaerobic respiration only and (ii) sequences upstream of genes displaying differences in transcript levels under aerobic respiration only. The top 30 candidate regulatory sites obtained between these runs corresponded with the sites identified by Gibbs sampling.

Figure 3 shows the DNA sequence logo (57) representing the potential regulatory motif generated from both computational motif searches based on the gene expression data. The predicted Fur-binding regulatory motif of *S. oneidensis* contains a 10-1-10 inverted repeat (palindrome). Those predicted regulatory sites showing agreement between the two computational methods used, along with their associated genes, are listed in Table 5. The majority of the genes belonged to the functional categories of hypothetical proteins or transport and binding proteins. The following genes encoding siderophore biosynthesis or transport functions exhibited strong induction patterns (in most cases, >5-fold increase in expression), as determined by DNA microarray analysis, and contained sites in their upstream regions matching the Fur motif model (posterior probabilities are given in parentheses): *ftn*, SO0139 (0.99); *bfd*, SO0583 (0.99); a putative TonB-dependent receptor, SO1482 (0.93); a TonB-dependent heme receptor, SO1580 (0.99); *feoA*, SO1783 (0.99); *alcA*, SO3030 (1.00); *hugA*, SO3669 (0.92); *tonB1*, SO3670 (0.92); and *irgA*, SO4523 (1.00). *feoA*, *alcA*, *hugA*, and *tonB1* are the first genes in the probable operons *feoAB*, *alcA*-SO3031-SO3032, *hugA*-SO3668-SO3667, and *tonB1-exbB1-exbD1*, respectively. Microarray experiments and DNA motif searches also implicated a number of genes with unknown functions as members of the Fur regulon, four of which are parts of probable operons not previously characterized (Table 5).

DISCUSSION

The advent of advanced analytical technologies, in particular DNA microarrays and high-performance liquid chromatography-tandem mass spectrometry, and sophisticated computational methods have enabled a detailed, global characterization of microbial cellular processes that had been unattainable before. In this study, we used targeted mutagenesis, genome-wide expression profiling, and an MS-based "gelless" method of proteome analysis to characterize the *S. oneidensis* Fur regulon and then to directly compare the regulon deduced from these genomic approaches with site predictions derived from computational methods for regulatory-motif discovery to make inferences about Fur regulation. Comparative global analysis of the transcriptomes for a *fur* deletion mutant (the FUR2 strain) and the parental (wild-type) strain indicated that ~11.5 and 9.7% of the total protein-encoding ORF content of *S. oneidensis* MR-1 displayed significant changes in expression under aerobic and anaerobic respiratory conditions, respectively, in complex LB medium. LB was selected as the growth medium for high-throughput functional genomic and proteomic studies because mid-log-phase OD growth yields (OD_{600} = 0.6) provided sufficient biomass to perform the required replications for microarray hybridization and LC-MS/MS analysis (see Materials and Methods). The growth of *S. oneidensis* parental and mutant strains in defined minimal medium containing physiologically relevant iron concentrations would have been preferred over LB, but it did not yield the required biomass in practical volumes for such high-throughput analyses (e.g., the mid-log-phase OD_{600} range observed for growth of the WT and *fur* mutant under aerobic and anaerobic conditions in M4 minimal medium was 0.02 to 0.1 [X.-F. Wan, J. Zhou, and D. K. Thomson, unpublished results]).

Most of the differentially expressed genes in the FUR2 strain were distributed among the functional role categories of energy metabolism, hypothetical proteins, and transport and binding proteins (Fig. 1), thus suggesting that a *fur* mutation has a pleiotropic effect on *S. oneidensis* gene expression. The search for Fur-binding regulatory motifs in the sequences upstream of coregulated genes suggested that Fur directly controls the transcription of possibly 39 genes, with 24 of these genes arranged in nine operons. This study found that 19 of the 39 predicted Fur-regulated genes encoded hypothetical or conserved hypothetical proteins and thus suggested, for the first time, a biological role for these genes in iron transport, assimilation, or iron stress response. Furthermore, proteomic analysis demonstrated the expression of two proteins encoded by previously annotated pseudogenes that showed increased abundance in FUR2 relative to the wild type.

The results described here are consistent with the primary function of *S. oneidensis* Fur as a repressor controlling siderophore- or receptor-mediated iron acquisition. Some of the most highly derepressed genes and operons were those with predicted functions in iron storage (*ftn*), siderophore biosynthesis (*alcA*-SO3031-SO3032) or uptake (*viuA*, *tonB1-exbB1-exbD1*, SO1482, SO3033, and SO4743), ferrous iron-hemin transport (*feoAB*, *hugA*, and *hmuTUV*), or other functions likely to be associated with iron acquisition and metabolism (*bfd* and *irgA*) (Table 1). To complement the DNA microarray

experiments, we performed computer-aided searches using the Gibbs Recursive Sampler and MOTIF REGRESSOR programs to identify potential regulatory motifs in the upstream regions of these highly induced genes with known functions. Strong candidate Fur-binding sites were discovered in the upstream regulatory regions of *ftn* (SO0139), *bfd* (SO0583), SO1482, SO1580, *feoA* (SO1783), *alcA* (SO3030), *hugA* (SO3669), *tonB1* (SO3670), *viuA* (SO4516), *irgA* (SO4523), and SO4743 (Table 5). Together, these data suggest that the *S. oneidensis* Fur regulon, defined here as those genes directly regulated by Fur, includes five operons (containing 13 genes) and 7 genes belonging to the functional category of transport and binding proteins. Although the identified *S. oneidensis* motif shows strong similarity to *E. coli* Fur sites in SCAN results and the 30 predicted sites from the gene expression data are unlikely to occur by chance alone, as shown with the Wilcoxon test, it is important to provide biochemical verification of these putative Fur-binding sites.

Based on the genome annotation, the gene cluster *tonB1-exbB1-exbD1* is one of two probable operons encoding a TonB transport system in *S. oneidensis*. In gram-negative bacteria, TonB-ExbB-ExbD systems utilize the proton motive force across the cytoplasmic membrane to transduce the energy required for outer membrane receptors and transporters to deliver ferri-siderophore complexes into the periplasmic space (49). While *E. coli* and most other gram-negative bacteria express a single TonB system, *Vibrio cholerae* (47) and *S. oneidensis* MR-1, whose protein-encoding ORFs are most similar to *V. cholerae* genes (32), encode two distinct TonB systems. The two TonB systems of *V. cholerae* have specific, as well as redundant, functions. While both systems can mediate the transport of hemin and certain siderophores, the *V. cholerae* TonB1 system specifically mediates utilization of the siderophore schizokinen, whereas the TonB2 complex of proteins is specifically required for enterobactin transport (58). Similarly, differences in genetic organization and transcript expression suggest that the TonB1 and TonB2 systems of *S. oneidensis* may possess unique functions as well and may be differentially regulated. DNA microarray analysis revealed that the *tonB1-exbB1-exbD1* operon showed high expression levels (17- to 39-fold) in the FUR2 strain, whereas the *exbB2-exbD2-tonB2* operon exhibited essentially no change in mRNA abundance in the FUR2 strain under conditions of available iron (Table 1). Furthermore, a strong candidate Fur-binding site was discovered upstream of the *tonB1* operon (Table 5) but not the *tonB2* operon, thus suggesting that Fur directly regulates transcription of the *tonB1* operon in response to intracellular iron levels. It is possible that the *S. oneidensis* TonB1 transport system may specifically mediate utilization of the uncharacterized siderophore synthesized by the protein product(s) encoded by the *alcA*-SO3031-SO3032 operon, which displays an induction range of 3- to13-fold under both aerobic and anaerobic growth conditions in the FUR2 strain (Table 1). Clearly, further research is needed to determine the functions of the two *S. oneidensis* TonB systems.

Both transcriptome and proteome analyses of the *S. oneidensis* FUR2 strain revealed a number of differentially expressed genes of unknown function, thus providing clues to their possible biological roles and regulation. Further analysis of these uncharacterized genes through the application of computational motif discovery methods suggested that the *S. oneidensis* Fur regulon includes four operons (containing 11 genes) and 8 genes encoding hypothetical or conserved hypothetical proteins (Table 5). Of those putative Fur-regulated genes with unknown functions exhibiting high-level expression (generally >10-fold) in the FUR2 strain, two operons (SO0447-SO0448-SO0449 and SO1188-SO1189-SO1190) and three genes (SO3062, SO3344, and SO4740) were predicted to encode membrane-associated proteins, based on the identification of two or more transmembrane helices (40). Genes SO2039 and SO3025, with undefined functions, were predicted to encode soluble proteins. Based on the gene expression data and the occurrence of strong Fur box-like motifs in their upstream regions, these operons and genes are likely to encode proteins, some perhaps unique to *S. oneidensis*, that function in siderophore biosynthesis or uptake, iron utilization, or other aspects of iron homeostasis.

In addition to genomic structural analysis and transcriptomic viewing through array technologies, proteomic analyses constitute an important component of functional genomic studies, because they enable the most essential level of gene expression to be visualized. Recently, *S. oneidensis* has been the focus of a number of proteome studies of different magnitudes that employed various technologies (5, 16, 25, 41, 63, 67, 69). In a previous study, a *fur* insertional mutant (FUR1) of *S. oneidensis* was compared with the wild-type strain by using 2D PAGE, followed by micro-LC-MS/MS (63). While this analysis revealed 11 major protein species exhibiting significant changes in abundance between the wild type and the *fur* mutant, only two of these proteins were from the expected class of transport and binding proteins, and many of the proteins showing large-scale differences in expression at the mRNA level by DNA microarray analysis were not identified. This may be due to the fact that typical 2D-PAGE methods have difficulty in capturing small proteins, proteins with widely ranging isoelectric points, and a large proportion of membrane-associated proteins.

To extend the protein identification to a more comprehensive level, we analyzed whole proteomes of aerobically grown wild-type and *fur* deletion strains by gelless qualitative shotgun MS proteomics. This method is very useful in rapidly determining large-scale protein differences between two samples but cannot identify exact changes and is insufficient to detect small changes in protein abundance. Variations of this qualitative methodology to determine changes in protein expression without isotopic labels have recently been proposed (10, 23). While these newer approaches may have the potential of giving more exact quantification, this was not the major focus of our study. Rather, we were interested in identifying proteins (mainly transporters, receptors, and binding proteins) predicted to be up-regulated in the *fur* deletion mutant by microarray analysis but yet predicted to be clearly identified by proteome analysis. Thus, we employed a very simple method to screen for proteins showing large differences in protein abundance between two biological samples by the percentage of sequence coverage and the number of peptides found across a triplicate measurement using three similar LC-MS/MS techniques.

Replicate whole-proteome analyses of aerobically grown WT and FUR2 strains resulted in the identification of a total of 1,104 proteins from both. Proteins showing dramatic changes in abundance (≥4 unique peptides and/or 30% sequence cov-

erage) were highlighted for comparison with the microarray data (Table 4). Of those induced genes likely to be members of the Fur regulon based on microarray and motif identification data, proteins encoded by SO0798 (a conserved hypothetical protein), SO1190 (a conserved hypothetical protein encoded by the SO1188-SO1189-SO1190 operon), SO1482 (a putative TonB-dependent receptor), SO1580 (a TonB-dependent heme receptor), SO3669 (a heme transport protein, HugA, encoded by part of the SO3669-SO3668-SO3667 operon), SO4516 (a ferric vibriobactin receptor, ViuA), SO4523 (an iron-regulated outer membrane virulence protein, IrgA), and SO4743 were identified by LC-MS/MS and showed significantly greater abundance in FUR2. Expression of two conserved hypothetical proteins, encoded by genes SO3667 and SO3668, was also up-regulated in the FUR2 strain, as demonstrated by LC-MS/MS analysis. Genes SO3667 and SO3668 are arranged together in a probable operon with *hugA* (SO3669) (Table 2). In this case as well, the in vivo abundance of these conserved hypothetical proteins was consistent with the observed increases in mRNA expression for the corresponding genes.

Other proteins detected in the large-scale proteome analysis had expression levels that inversely correlated with the transcriptome data (Table 4). An ornithine decarboxylase (SO0314), a heavy-metal efflux pump (SO0520), alkyl hydroperoxidase reductase (SO0958), and uridine phosphorylase (SO4133), for example, showed increased abundances in FUR2, while their corresponding transcript levels were slightly down-regulated, as identified by microarray hybridization. While this lack of one-to-one correlation between the proteomics and microarray data may be somewhat surprising, it is important to keep in mind that protein stability, modifications, and/or turnover may alter the protein abundances expected from the microarray data (12, 21, 50). In addition, it is not clear why the expression of these proteins would be affected by a *fur* deletion, although differences in their expression may be related more to the cell's attempt to cope with high intracellular iron levels in the absence of a functional Fur regulator. The inconsistencies between the transcriptome and proteome data sets emphasize the importance of investigating gene expression from the perspectives of both transcription and translation to account for the different levels of regulation possible in prokaryotes. A significant finding that emerged from the proteomic analysis was the identification of protein products encoded by genes originally annotated in the *S. oneidensis* MR-1 genome published by Heidelberg et al. (32) as having authentic point mutations or frameshifts, i.e., as pseudogenes.

Consistent with a previous study (63), the *fur* deletion affected the transcription of *S. oneidensis* genes with annotated functions in energy metabolism (Fig. 1). In cells harboring a *fur* deletion mutation, expression of both *omcA* and *omcB*, which resides immediately downstream of *omcA* on the genome, was repressed under the two respiratory conditions tested (Table 1). The decrease in *omcA* and *omcB* expression at the transcript level correlated well with the apparent absence of the OmcA and OmcB proteins in FUR2 under aerobic growth conditions (Table 4). Cytochromes OmcA and OmcB contain *c*-type hemes and are localized to the outer membrane of *S. oneidensis* (43). A study by Myers and Myers (44) indicated a role for OmcA and OmcB in the anaerobic reduction of MnO_2 by *S. oneidensis*. Recently, evidence that these outer membrane cytochromes are cell surface exposed suggests that OmcA and OmcB may directly contact extracellular metal oxides at the cell surface (42). Other than cytochrome *c* oxidase (SO2363), these were the only cytochromes showing significant changes in protein abundance based on LC-MS/MS analysis. Very little is known about the expression and regulation of *omcA* and *omcB*, with the exception that *omcA* showed increased expression in *S. oneidensis* cells exposed to a shift from aerobic growth to anaerobic growth in the presence of fumarate, Fe(III), or nitrate (5).

Along with the measured decreases in mRNA and protein abundance for *omcA* and *omcB*, a potential Fur regulatory site with a posterior probability of 0.97 was discovered upstream of *omcA* (SO1779) at position −43 relative to the predicted translation start codon (Table 5). This site was identified using both computational methods, Gibbs Recursive Sampler and MOTIF REGRESSOR, and is particularly intriguing because it lies upstream of a gene that appears to be a direct target of Fur-mediated activation, based on gene expression profiling. Previously, *E. coli* genes encoding succinate dehydrogenase of the tricarboxylic acid cycle, ferritin, and manganese-cofactored superoxide dismutase were shown to be positively regulated by Fur by an unknown mechanism. Similarly, studies have shown that transcript and protein expression levels for an Fe-cofactored superoxide dismutase (encoded by *sodB* [SO2881]) are reduced in a *fur* mutant (Table 1), thus suggesting that positive regulation by Fur may be operating in *S. oneidensis* as well (reference 63 and this study).

A recent investigation by Massé and Gottesman (38) demonstrated that *E. coli* Fur positively regulates intracellular iron use and storage indirectly by repressing expression of a small RNA, RyhB, in the presence of iron. RyhB appears to act as an antisense RNA, down-regulating iron storage proteins and nonessential iron-containing proteins under iron-limiting conditions (38). ClustalW multiple alignments between the *ryhB* Rfam (http://rfam.wustl.edu/) seed sequences and the *S. oneidensis* MR-1 sequence from genome coordinates 4920241 to 4920347 revealed a region of strong conservation (data not shown), suggesting that this MR-1 sequence may be a *ryhB*-like gene. In addition, the MR-1 sequence is located downstream of gene SO4716, which is an ortholog of the *V. cholerae* gene VC0106. The *ryhB* gene in *V. cholerae* is also located downstream of VC0106. Thus, the *S. oneidensis* region between 4920241 and 4920347 has both homology and synteny with *V. cholerae*. Further research is needed to ascertain whether *S. oneidensis* Fur mediates positive regulation through repression of a *ryhB* homolog and/or whether it can function as an activator in certain cases by directly binding to its recognition site upstream of genes such as *omcA*. Future research will focus on experimentally verifying the functionality of predicted Fur-binding regulatory motifs and the involvement of Fur regulation in *S. oneidensis* energy metabolism.

ACKNOWLEDGMENTS

We thank Xiaohe Shirley Liu and Jun Liu from Harvard University and Maria Ermolaeva from TIGR for their assistance with some of the data analysis. We also acknowledge Ting Li for technical help with microarray hybridization. We also thank Charles E. Lawrence for advice and critical comments on the statistical analysis of microarray data. We thank Goran Mitulovic, Mark Van Gils, and LC Packings, a Dionex Company, for providing and helping in optimizing the 2D

HPLC system used in this study. We thank the Grace Vydac Corp. for providing the HPLC columns through a collaborative agreement. We also thank David Tabb and the John Yates Proteomics Laboratory at Scripps Research Institute for DTASelect and Contrast software. F. W. Larimer and M. Land of the ORNL Genome Analysis and System Modeling Group provided the combined ORNL-TIGR annotated proteome database used for all proteome studies.

N. C. VerBerkmoes and H. Connelly acknowledge support from the University of Tennessee (Knoxville)-ORNL Graduate School of Genome Science and Technology. This research was funded by U.S. Department of Energy (Office of Biological and Environmental Research, Office of Science) grants from the Genomies:GTL and Microbial Genome Programs. Oak Ridge National Laboratory is managed by University of Tennessee-Battelle LLC for the Department of Energy under contract DOE-AC05-00OR22725.

REFERENCES

1. **Andrews, S. C., A. K. Robinson, and F. Rodríguez-Quiñones.** 2003. Bacterial iron homeostasis. FEMS Microbiol. Rev. **27:**215–237.
2. **Badger, J. H., and G. J. Olsen.** 1999. CRITICA: coding region identification tool invoking comparative analysis. Mol. Biol. Evol. **16:**512–524.
3. **Bagg, A., and J. B. Neilands.** 1987. Ferric uptake regulation protein acts as a repressor, employing iron(II) as a cofactor to bind the operator of an iron transport operon in *Escherichia coli.* Biochemistry **26:**5471–5477.
4. **Beliaev, A. S., and D. A. Saffarini.** 1998. *Shewanella putrefaciens mtrB* encodes an outer membrane protein required for Fe(III) and Mn(IV) reduction. J. Bacteriol. **180:**6292–6297.
5. **Beliaev, A. S., D. K. Thompson, T. Khare, H. Lim, C. C. Brandt, G. Li, A. E. Murray, J. F. Heidelberg, C. S. Giometti, J. Yates III, K. H. Nealson, J. M. Tiedje, and J. Zhou.** 2002. Gene and protein expression profiles of *Shewanella oneidensis* during anaerobic growth with different electron acceptors. OMICS **6:**39–60.
6. **Bereswill, S., S. Greiner, A. H. M. Van Vliet, B. Waidner, F. Fassbinder, E. Schiltz, J. G. Kusters, and M. Kist.** 2000. Regulation of ferritin-mediated cytoplasmic iron storage by the ferric uptake regulator homolog (Fur) of *Helicobacter pylori.* J. Bacteriol. **182:**5948–5953.
7. **Berish, S. A., S. Subbarao, C.-Y. Chen, D. L. Trees, and S. A. Morse.** 1993. Identification and cloning of a *fur* homolog from *Neisseria gonorrhoeae.* Infect. Immun. **61:**4599–4606.
8. **Bijlsma, J. J. E., B. Waidner, A. H. M. Van Vliet, N. J. Hughes, S. Häg, S. Bereswill, D. J. Kelly, C. M. J. E. Vandenbroucke-Grauls, M. Kist, and J. G. Kusters.** 2002. The *Helicobacter pylori* homologue of the ferric uptake regulator is involved in acid resistance. Infect. Immun. **70:**606–611.
9. **Bsat, N., A. Herbig, L. Casillas-Martinez, P. Setlow, and J. D. Helmann.** 1998. *Bacillus subtilis* contains multiple Fur homologues: identification of the iron uptake (Fur) and peroxide regulon (PerR) repressors. Mol. Microbiol. **29:**189–198.
10. **Chelius, D., and P. V. Bondarenko.** 2002. Quantitative profiling of proteins in complex mixtures using liquid chromatography and mass spectrometry. J. Proteome Res. **1:**317–323.
11. **Conlon, E. M., X. S. Liu, J. D. Lieb, and J. S. Liu.** 2003. Integrating regulatory motif discovery and genome-wide expression analysis. Proc. Natl. Acad. Sci. USA **100:**3339–3344.
12. **Corbin, R. W., O. Paliy, F. Yang, J. Shabanowitz, M. Platt, C. E. Lyons, Jr., K. Root, J. McAuliffe, M. I. Jordan, S. Kustu, E. Soupene, and D. F. Hunt.** 2003. Toward a protein profile of *Escherichia coli*: comparison to its transcription profile. Proc. Natl. Acad. Sci. USA **100:**9232–9237.
13. **Delcher, A. L., D. Harmon, S. Kasif, O. White, and S. L. Salzberg.** 1999. Improved microbial gene identification with GLIMMER. Nucleic Acids Res. **27:**4636–4641.
14. **de Lorenzo, V., S. Wee, M. Herrero, and J. B. Neilands.** 1987. Operator sequences of the aerobactin operon of plasmid ColV-K30 binding the ferric uptake regulation (*fur*) repressor. J. Bacteriol. **169:**2624–2630.
15. **de Lorenzo, V., F. Giovannini, M. Herrero, and J. B. Neilands.** 1988. Metal ion regulation of gene expression. Fur repressor-operator interaction at the promoter region of the aerobactin system of pColV-K30. J. Mol. Biol. **203:**875–884.
16. **Devreese, B., F. Vanrobaeys, and J. Van Beeumen.** 2001. Automated nanoflow liquid chromatography/tandem mass spectrometric identification of proteins from *Shewanella putrefaciens* separated by two-dimensional polyacrylamide gel electrophoresis. Rapid Commun. Mass Spectrom. **15:**50–56.
17. **DiGiuseppe, P. A., and T. J. Silhavy.** 2003. Signal detection and target gene induction by the CpxRA two-component system. J. Bacteriol. **185:**2432–2440.
18. **Eng, J. K., A. L. McCormack, and J. R. Yates III.** 1994. An approach to correlate tandem mass spectral data of peptides with amino acid sequences in a protein database. J. Am. Mass Spectrom. **5:**976–989.
19. **Ermolaeva, M. D., O. White, and S. L. Salzberg.** 2001. Prediction of operons in microbial genomes. Nucleic Acids Res. **29:**1216–1221.
20. **Escolar, L., J. Pérez-Martín, and V. de Lorenzo.** 1999. Opening the iron box: transcriptional metalloregulation by the Fur protein. J. Bacteriol. **181:**6223–6229.
21. **Eymann, C., G. Homuth, C. Scharf, and M. Hecker.** 2002. *Bacillus subtilis* functional genomics: global characterization of the stringent response by proteome and transcriptome analysis. J. Bacteriol. **184:**2500–2520.
22. **Foster, J. W., and H. K. Hall.** 1992. Effect of *Salmonella typhimurium* ferric uptake regulator (*fur*) mutations on iron- and pH-regulated protein synthesis. J. Bacteriol. **174:**4317–4323.
23. **Gao, J., G. J. Opiteck, M. Friedrichs, A. R. Dongre, and S. A. Hefta.** 2003. Changes in the protein expression of yeast as a function of carbon source. J. Proteome Res. **2:**643–649.
24. **Ghassemian, M., and N. A. Straus.** 1996. Fur regulates the expression of iron-stress genes in the cyanobacterium *Synechococcus* sp. strain PCC7942. Microbiology **142:**1469–1476.
25. **Giometti, C. S., T. Khare, S. L. Tollaksen, A. Tsapin, W. Zhu, J. R. Yates III, and K. H. Nealson.** 2003. Analysis of the *Shewanella oneidensis* proteome by two-dimensional gel electrophoresis under nondenaturing conditions. Proteomics **3:**777–785.
26. **Hantke, K.** 1987. Ferrous iron transport mutants in *Escherichia coli* K12. FEMS Microbiol. Lett. **44:**53–57.
27. **Hantke, K.** 2001. Iron and metal regulation in bacteria. Curr. Opin. Microbiol. **4:**172–177.
28. **Hassan, H. M., and H.-C. H. Sun.** 1992. Regulatory roles of Fnr, Fur, and Arc in expression of manganese-containing superoxide dismutase in *Escherichia coli.* Proc. Natl. Acad. Sci. USA **89:**3217–3221.
29. **Hassett, D. J., M. L. Howell, U. A. Ochsner, M. L. Vasil, Z. Johnson, and G. E. Dean.** 1997. An operon containing *fumC* and *sodA* encoding fumarase C and manganese superoxide dismutase is controlled by the ferric uptake regulator in *Pseudomonas aeruginosa*: *fur* mutants produce elevated alginate levels. J. Bacteriol. **179:**1452–1459.
30. **Hassett, D. J., P. A. Sokol, M. L. Howell, J.-F. Ma, H. T. Schweizer, U. Ochsner, and M. L. Vasil.** 1996. Ferric uptake regulator (Fur) mutants of *Pseudomonas aeruginosa* demonstrate defective siderophore-mediated iron uptake, altered aerobic growth, and decreased superoxide dismutase and catalase activities. J. Bacteriol. **178:**3996–4003.
31. **Hegde, P., R. Qi, K. Abernathy, C. Gay, S. Dharap, R. Gaspard, J. E. Hughes, E. Snesrud, N. Lee, and J. Quackenbush.** 2000. A concise guide to cDNA microarray analysis. BioTechniques **29:**548–562.
32. **Heidelberg, J. F., I. T. Paulsen, K. E. Nelson, E. J. Gaidos, W. C. Nelson, T. D. Read, J. A. Eisen, R. Seshadri, N. Ward, B. Methe, R. A. Clayton, T. Meyer, A. Tsapin, J. Scott, M. Beanan, L. Brinkac, S. Daugherty, R. T. DeBoy, R. J. Dodson, A. S. Durkin, D. H. Haft, J. F. Kolonay, R. Madupu, J. D. Peterson, L. A. Umayam, O. White, A. M. Wolf, J. Vamathevan, J. Weidman, M. Impraim, K. Lee, K. Berry, C. Lee, J. Mueller, H. Khouri, J. Gill, T. R. Utterback, L. A. McDonald, T. V. Feldblyum, H. O. Smith, J. C. Venter, K. H. Nealson, and C. M. Fraser.** 2002. Genome sequence of the dissimilatory metal ion-reducing bacterium *Shewanella oneidensis.* Nat. Biotechnol. **20:**1118–1123.
33. **Kalogeraki, V. S., and S. C. Winans.** 1997. Suicide plasmids containing promoterless reporter genes can simultaneously disrupt and create fusions to target genes of diverse bacteria. Gene **188:**69–75.
34. **Karjalainen, T. K., D. G. Evans, D. J. Evans, D. Y. Graham, Jr., and C. H. Lee.** 1991. Iron represses the expression of CFA/I fimbriae of enterotoxigenic *E. coli.* Microb. Pathog. **11:**317–323.
35. **Lawrence, C. E., S. F. Altschul, M. S. Boguski, J. S. Liu, A. F. Neuwald, and J. C. Wootton.** 1993. Detecting subtle sequence signals: a Gibbs sampling strategy for multiple alignment. Science **262:**208–214.
36. **Link, A. J., D. Phillips, and G. M. Church.** 1997. Methods for generating precise deletions and insertions in the genome of wild-type *Escherichia coli*: application to open reading frame characterization. J. Bacteriol. **179:**6228–6237.
37. **Litwin, C. M., S. A. Boyko, and S. B. Calderwood.** 1992. Cloning, sequencing, and transcriptional regulation of the *Vibrio cholerae fur* gene. J. Bacteriol. **174:**1897–1903.
38. **Massé, E., and S. Gottesman.** 2002. A small RNA regulates the expression of genes involved in iron metabolism in *Escherichia coli.* Proc. Natl. Acad. Sci. USA **99:**4620–4625.
39. **Miller, V. L., and J. J. Mekalanos.** 1988. A novel suicide vector and its use in construction of insertion mutations: osmoregulation of outer membrane proteins and virulence determinants in *Vibrio cholerae* requires *toxR.* J. Bacteriol. **170:**2575–2583.
40. **Mitaku, S., T. Hirokawa, and T. Tsuji.** 2002. Amphiphilicity index of polar amino acids as an aid in the characterization of amino acid preference at membrane-water interfaces. Bioinformatics **18:**608–616.
41. **Mohan, D., L. Paša-Tolić, C. D. Masselon, N. Tolić, B. Bogdanov, K. K. Hixson, R. D. Smith, and C. S. Lee.** 2003. Integration of electrokinetic-based multidimensional separation/concentration platform with electrospray ionization-Fourier transform ion cyclotron resonance-mass spectrometry for proteome analysis of *Shewanella oneidensis.* Anal. Chem. **75:**4432–4440.
42. **Myers, C. R., and J. M. Myers.** 2003. Cell surface exposure of the outer membrane cytochromes of *Shewanella oneidensis* MR-1. Lett. Appl. Microbiol. **37:**254–258.

43. **Myers, C. R., and J. M. Myers.** 1992. Localization of cytochromes to the outer membrane of anaerobically grown *Shewanella putrefaciens* MR-1. J. Bacteriol. **174:**3429–3438.
44. **Myers, J. M., and C. R. Myers.** 2001. Role for outer membrane cytochromes OmcA and OmcB of *Shewanella putrefaciens* MR-1 in reduction of manganese dioxide. Appl. Environ. Microbiol. **67:**260–269.
45. **Neuwald, A. F., J. S. Liu, and C. E. Lawrence.** 1995. Gibbs motif sampling: detection of bacterial outer membrane protein repeats. Protein Sci. **4:**1618–1632.
46. **Niederhoffer, E. C., C. M. Naranjo, K. L. Bradley, and J. A. Fee.** 1990. Control of *Escherichia coli* superoxide dismutase (*sodA* and *sodB*) genes by the ferric uptake regulation (*fur*) locus. J. Bacteriol. **172:**1930–1938.
47. **Occhino, D. A., E. E. Wyckoff, D. P. Henderson, T. J. Wrona, and S. M. Payne.** 1998. *Vibrio cholerae* iron transport: haem transport genes are linked to one of two sets of *tonB*, *exbB*, *exbD* genes. Mol. Microbiol. **29:**1493–1507.
48. **Pohl, E., J. C. Haller, A. Mijovilovich, W. Meyer-Klaucke, E. Garman, and M. L. Vasil.** 2003. Architecture of a protein central to iron homeostasis: crystal structure and spectroscopic analysis of the ferric uptake regulator. Mol. Microbiol. **47:**903–915.
49. **Postle, K., and R. J. Kadner.** 2003. Touch and go: tying TonB to transport. Mol. Microbiol. **49:**869–882.
50. **Pratt, J. M., J. Petty, I. Riba-Garcia, D. H. L. Robertson, S. J. Gaskell, S. G. Oliver, and R. J. Beynon.** 2002. Dynamics of protein turnover, a missing dimension in proteomics. Mol. Cell. Proteomics **1:**579–591.
51. **Prince, R. W., C. D. Cox, and M. L. Vasil.** 1993. Coordinate regulation of siderophore and exotoxin A production: molecular cloning and sequencing of the *Pseudomonas aeruginosa fur* gene. J. Bacteriol. **175:**2589–2598.
52. **Ratledge, C., and L. G. Dover.** 2000. Iron metabolism in pathogenic bacteria. Annu. Rev. Microbiol. **54:**881–941.
53. **Ried, J. L., and A. Collmer.** 1987. An *nptI-sacB-sacR* cartridge for constructing directed, unmarked mutations in gram-negative bacteria by marker exchange-eviction mutagenesis. Gene **57:**239–246.
54. **Saffarini, D. A., and K. H. Nealson.** 1993. Sequence and genetic characterization of *etrA*, an *fnr* analog that regulates anaerobic respiration in *Shewanella putrefaciens* MR-1. J. Bacteriol. **175:**7938–7944.
55. **Salzberg, S. L., A. L. Delcher, S. Kasif, and O. White.** 1998. Microbial gene identification using interpolated Markov models. Nucleic Acids Res. **26:**544–548.
56. **Schena, M., D. Shalon, R. Heller, A. Chai, P. O. Brown, and R. W. Davis.** 1996. Parallel human genome analysis: microarray-based expression monitoring of 1000 genes. Proc. Natl. Acad. Sci. USA **93:**10614–10619.
57. **Schneider, T. D., and R. M. Stephens.** 1990. Sequence logos: a new way to display consensus sequences. Nucleic Acids Res. **18:**6097–6100.
58. **Seliger, S. S., A. R. Mey, A.-M. Valle, and S. M. Payne.** 2001. The two TonB systems of *Vibrio cholerae*: redundant and specific functions. Mol. Microbiol. **39:**801–812.
59. **Stojiljkovic, I., A. J. Bäumer, and K. Hantke.** 1994. Fur regulon in gram-negative bacteria. J. Mol. Biol. **236:**531–545.
60. **Tabb, D. L., W. Hayes-McDonald, and J. R. Yates.** 2002. DTASelect and contrast: tools for assembling and comparing protein identifications from shotgun proteomics. J. Proteome Res. **1:**21–26.
61. **Thomas, C. E., and P. F. Sparling.** 1994. Identification and cloning of a *fur* homolog from *Neisseria meningitidis.* Mol. Microbiol. **11:**725–737.
62. **Thomas, C. E., and P. F. Sparling.** 1996. Isolation and analysis of a *fur* mutant of *Neisseria gonorrhoeae.* J. Bacteriol. **178:**4224–4232.
63. **Thompson, D. K., A. S. Beliaev, C. S. Giometti, S. L. Tollaksen, T. Khare, D. P. Lies, K. H. Nealson, H. Lim, J. Yates III, C. C. Brandt, J. M. Tiedje, and J. Zhou.** 2002. Transcriptional and proteomic analysis of a ferric uptake regulator (Fur) mutant of *Shewanella oneidensis*: possible involvement of Fur in energy metabolism, transcriptional regulation, and oxidative stress. Appl. Environ. Microbiol. **68:**881–892.
64. **Thompson, W., E. C. Rouchka, and C. E. Lawrence.** 2003. Gibbs Recursive Sampler: finding transcription factor binding sites. Nucleic Acids Res. **31:**3580–3585.
65. **Tolmasky, M. E., A. M. Wertheimer, L. A. Actis, and J. H. Crosa.** 1994. Characterization of the *Vibrio anguillarum fur* gene: role in regulation of expression of the FatA outer membrane protein and catechols. J. Bacteriol. **176:**213–220.
66. **Touati, D.** 2000. Iron and oxidative stress in bacteria. Arch. Biochem. Biophys. **373:**1–6.
67. **Vanrobaeys, F., B. Devreese, E. Lecocq, L. Rychlewski, L. De Smet, and J. Van Beeumen.** 2003. Proteomics of the dissimilatory iron-reducing bacterium *Shewanella oneidensis* MR-1, using a matrix-assisted laser desorption/ionization-tandem-time of flight mass spectrometer. Proteomics **3:**2249–2257.
68. **Venturi, V., C. Ottevanger, M. Bracke, and P. Weisbeek.** 1995. Iron regulation of siderophore biosynthesis and transport in *Pseudomonas putida* WCS358: involvement of a transcriptional activator and of the Fur protein. Mol. Microbiol. **15:**1081–1093.
69. **VerBerkmoes, N. C., J. L. Bundy, L. Hauser, K. G. Asano, J. Razumovskaya, F. Larimer, R. L. Hettich, and J. L. Stephenson, Jr.** 2002. Integrating "Top-Down" and "Bottom-Up" mass spectrometric approaches for proteomic analysis of *Shewanella oneidensis.* J. Proteome Res. **1:**239–252.
70. **Xiong, A., V. K. Singh, G. Cabrera, and R. K. Jayaswal.** 2000. Molecular characterization of the ferric-uptake regulator, Fur, from *Staphylococcus aureus.* Microbiology **146:**659–668.
71. **Xu, D., G. Li, L. Wu, J. Zhou, and Y. Xu.** 2002. PRIMEGENS: robust and efficient design of gene-specific probes for microarray analysis. Bioinformatics **18:**1432–1437.
72. **Zhou, J.-Z., M. E. Davey, J. B. Figueras, E. Rivkina, D. Gilichinsky, and J. M. Tiedje.** 1997. Phylogenetic diversity of a bacterial community determined from Siberian tundra soil DNA. Microbiology **143:**3913–3919.